TNCME: TENSOR'S NORM CONSTRAINTS FOR UNSUPERVISED CONTRASTIVE LEARNING OF MULTIMODAL EMBEDDINGS

Anonymous authors
Paper under double-blind review

ABSTRACT

Multimodal embedding representation has emerged as a hot research topic and has been applied to multimodal retrieval tasks. Unsupervised contrastive learning, represented by InfoNCE, serves as the mainstream training paradigm for multimodal retrieval tasks. However, existing methods generally only optimize the directional alignment of positive pairs in the embedding space, and neglect another fundamental property of the representation tensors: magnitude. Based on this intuitive insight, we propose a **T**ensor's **N**orm **C**onstraints of **M**ultimodal **E**mbeddings framework, TNCME, which focuses on aligning the 2-norm of embedding representations between positive pairs during contrastive learning, jointly trained with the directional alignment pursued by InfoNCE. This approach optimizes the Top-1 performance of visual-language models in multimodal retrieval tasks. We first rigorously prove that the training objective of norm alignment of representations is consistent with the training logic of contrastive learning, and then adapt this objective to multimodal retrieval tasks. Based on the VLM2Vec-V2 framework, we perform training and evaluation across a total of 81 tasks spanning three representative multimodal retrieval categories: Image-Text, VisDoc-Text, and Video-Text. Experimental results demonstrate that the proposed TNCME outperforms baseline methods across all Top-1 metrics. Code open-sourced on anonymously GitHub: `https://anonymous.4open.science/r/TNCME-ICLR/`

1 INTRODUCTION

In multimodal retrieval tasks, existing approaches are primarily categorized into two main groups. The first group includes dual-tower architectures, such as CLIP (Radford et al., 2021a), BridgeTower (Xu et al., 2023b), and ManagerTower (Xu et al., 2023a), which encode images and text independently, often using CLIP-ViT and RoBERTa (Liu et al., 2019), and suffer from limited cross-modal interaction and fine-grained semantic alignment. The second group comprises some Vision-Language Models (VLMs) such as LLaVA (Liu et al., 2023a; 2024a;b) and the Qwen-VL series (Bai et al., 2023; Wang et al., 2025b), which adopt a "ViT-Projector-LLM" architecture to inject visual features into large language models (LLMs) via a projector. These models achieve more powerful modal alignment, contextual understanding, and semantic reasoning, making VLM-based representation learning an emerging trend in multimodal retrieval tasks.

Although VLM2Vec(Jiang et al., 2025) and VLM2Vec-V2(Meng et al., 2025) have preliminarily demonstrated the feasibility of applying multimodal retrieval tasks to VLMs, these methods still rely on InfoNCE(van den Oord et al., 2018) as the sole training objective, lacking a refined modeling of the multimodal alignment process. InfoNCE normalizes representations to focus training on directional alignment within a unit hypersphere: bringing positive pairs closer while pushing soft negative pairs more uniform. However, this mechanism has inherent limitations—when semantically mismatched visual-text pairs exhibit similar directions, the model may struggle to distinguish them effectively, thereby weakening its discriminative capability. The issue reveals the limitations of relying solely on directional alignment, prompting us to further focus on another key attribute of representation vectors—magnitude. In this work, we consider the magnitude of semantic representations as their L2 norm. Magnitude reflects the "energy" intensity of embedding vectors in the

feature space, serving as a crucial dimension for characterizing the semantic density and saliency of samples. Unlike cosine similarity, which measures only directional similarity, norm reveals more nuanced distribution characteristics of samples in high-dimensional space. For instance, semantically rich or visually salient images or texts may exhibit larger norms. Thus, imposing norm alignment constraints during training tightens both directional and norm alignment of positive samples, directly boosting Top-1 retrieval performance, as shown in Fig. 1. TNCSE(Zong et al., 2025) improves upon SimCSE(Gao et al., 2021) in semantic textual similarity tasks by introducing a norm alignment constraint on semantic representation tensors, demonstrating the importance of norm alignment in sentence representation learning. Building upon this, we propose integrating norm alignment into a multimodal contrastive learning framework to establish a more comprehensive mechanism for representation alignment. We further propose TNCME, a novel multimodal embedding framework that jointly optimizes directional alignment and norm consistency to enhance positive-pair matching in magnitude while preserving InfoNCE's directional modeling, improving generalization in multimodal retrieval.

To our knowledge, no existing work has conducted a rigorous theoretical analysis of the semantic tensor norm alignment training objective. This objective neither clarifies whether the optimization process aligns with expected logic nor explores the existence of multiple local optima, making it difficult to guarantee convergence stability and alignment consistency. Furthermore, TNCSE is designed for pure text unimodal scenarios, where hidden states encoded by BERT-like models(Devlin et al., 2019; Liu et al., 2019; Reimers & Gurevych, 2019) exhibit slight variation in their norm distributions. In contrast, multimodal tasks involve significant differences in semantic representations between visual and textual from the outset—not only in direction but also in norm scales. Therefore, directly transferring TNCSE's norm alignment objective to multimodal scenarios may lead to training instability or performance degradation. To address these challenges, we first conduct a rigorous theoretical derivation of the training objective for norm alignment, which proves that the designed optimization objective possesses a globally optimal solution, thereby avoiding optimization difficulties caused by multiple local maxima and enhancing the interpretability of the training process. Simultaneously, we verify that the loss function's update direction aligns with the desired norm alignment trend, demonstrating that this mechanism effectively guides positive samples toward consistency in the representation space. Building upon this foundation, we refine the original norm alignment objective to enhance the model's robustness to multimodal feature discrepancies, making it more suitable for the demands of multimodal contrastive learning, which ultimately enables the collaborative optimization of both direction and norm for query-target embedding pairs of positive samples, leading to an improvement of Top-1 retrieval performance.

We implement training and evaluation of the visual-text retrieval task on the Qwen2-VL-2B model with the VLM2Vec-V2 framework. First, we locally reproduce VLM2Vec-Qwen2-VL-2B as the baseline model to ensure consistency in the experimental environment and comparability of results. Subsequently, based on the proposed TNCME framework, we train the improved model, TNCME-Qwen2-VL-2B, and compare it with the baseline under an identical testing environment. Experimental results demonstrate that across 36 image-text retrieval tasks, 27 visdoc-text tasks, and 18 video tasks, TNCME-Qwen2-VL-2B outperforms baseline on multiple key metrics, including Hit, NDCG, Precision, F1, Recall, MAP, and MRR, which fully validates the effectiveness and generalization capability of the proposed method in enhancing multimodal retrieval performance. Furthermore, ablation experiments are conducted to validate the rationality of modifying the tensor norm constraint in the training objective. Visualizations of sample embeddings in two-dimensional space reveal that under norm alignment, the query and target distributions of positive samples converge more closely, indicating that this training objective better aligns with retrieval task requirements.

We summarize the main contributions of this work as follows:

- To our knowledge, we are the first to introduce the concept of norm alignment for semantic representation tensors into multimodal unsupervised contrastive learning, proposing the multimodal embedding framework TNCME and applying it to multimodal retrieval tasks.
- Through rigorous mathematical proof, we demonstrate that the training objective for norm-aligned alignment possesses a unique optimal solution, and we visually illustrate the trend of this loss function.
- Training and evaluation are conducted within the VLM2Vec-V2 framework. We validate the effectiveness of the proposed method across 36 image-text retrieval tasks, 27 VisDoc-

text retrieval tasks, and 18 video-text retrieval tasks. The results demonstrate improvements across all benchmarks in the Top-1 metrics, indicating more significant precision at the highest ranking position.

2 Related Works

Before the ViT-Proj-LLM architecture, CLIP(Radford et al., 2021a) pioneered visual-language alignment using the InfoNCE loss, which enforces directional consistency between image and text embeddings for efficient cross-modal alignment. Subsequent models, such as BLIP(Li et al., 2022) and BLIP-2(Li et al., 2023), introduced cross-attention to enable early multimodal feature fusion, thereby enhancing intermodal interaction and contrastive learning efficacy. BridgeTower(Xu et al., 2023b) and ManagerTower(Xu et al., 2023a) further improved fine-grained alignment via structural optimizations, which still relied primarily on InfoNCE. With the rise of ViT-Proj-LLM architectures, visual-language alignment has transitioned from complex cross-attention to simpler, more efficient feedforward networks. Under this paradigm, Both GME(Zhang et al., 2024) and LamRA(Liu et al., 2025) explore the application of unsupervised contrastive learning in multimodal retrieval tasks. VLM2Vec(Jiang et al., 2025) introduces the MMEB benchmark(Meng et al., 2025) and applies unsupervised contrastive fine-tuning on Phi-3.5-V(Abdin et al., 2024), boosting training efficiency and representation quality via GradCache. VLM2Vec-V2(Meng et al., 2025) introduces a more comprehensive benchmark, MMEB-V2, and employs Qwen2VL(Wang et al., 2025b) as its backbone. According to the VLM2Vec-V2 report, which outperforms mainstream open-source approaches in the MMEB-V2 benchmark.

3 Method

In this section, we review the tensor norm constraint as a training objective for semantic representations in unsupervised contrastive learning and demonstrate its alignment with the principles of contrastive learning. We then introduce our core method, the multimodal embedding framework TNCME, detailing how it integrates tensor norm constraints with InfoNCE loss for joint training.

3.1 Review of Tensor Norm Constraint Training Objectives

In multimodal retrieval tasks, existing unsupervised contrastive learning methods typically employ InfoNCE loss to learn embeddings by modeling the semantic representation directions of positive and negative sample pairs in hyperspherical space. TNCSE has demonstrated that focusing on the 2-norm of the representation tensor can optimize the performance of BERT-like models in semantic text similarity tasks. Our objective is to prove the effectiveness of this approach and apply it to multimodal retrieval tasks. Therefore, we first briefly review the training objective of the semantic representation tensor 2-norm constraint.

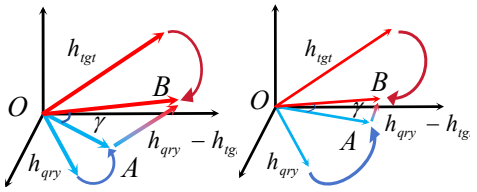

(a) Direction only constrainted. (b) Direction and norm are jointly constrained.

Figure 1: These two subfigures illustrate the advantages of norm alignment and direction alignment in three-dimensional space.

If $\mathbf{h}_{qry}$ and $\mathbf{h}_{tgt}$ denote the representations of positive samples in a contrastive learning pair, the tensor norm constraint training objective is defined as Eq. 1:

$$L_{TN}\left(\mathbf{h}_{qry}, \mathbf{h}_{tgt}\right) = \frac{\|\mathbf{h}_{qry} - \mathbf{h}_{tgt}\|}{\|\mathbf{h}_{qry}\| + \|\mathbf{h}_{tgt}\|}, \tag{1}$$

where $\|\cdot\|$ denotes the 2-norm of the tensor. Reducing the high-dimensional semantic representations to a three-dimensional space for visualization, as shown in Fig. 1, it is evident that we can perform vector subtraction on $\mathbf{h}_{qry}$ and $\mathbf{h}_{tgt}$. Since all tensors in Eq. 1 have been normalized to the 2-norm, we obtain a triangle $\triangle OAB$. Expanding the numerator using the cosine theorem gives Eq. 2:

$$L_{TN}\left(\mathbf{h}_{qry}, \mathbf{h}_{tgt}\right) = \frac{\sqrt{\|\mathbf{h}_{qry}\|^2 + \|\mathbf{h}_{tgt}\|^2 - 2\|\mathbf{h}_{qry}\|\|\mathbf{h}_{tgt}\|\cos\gamma}}{\|\mathbf{h}_{qry}\| + \|\mathbf{h}_{tgt}\|}, \tag{2}$$

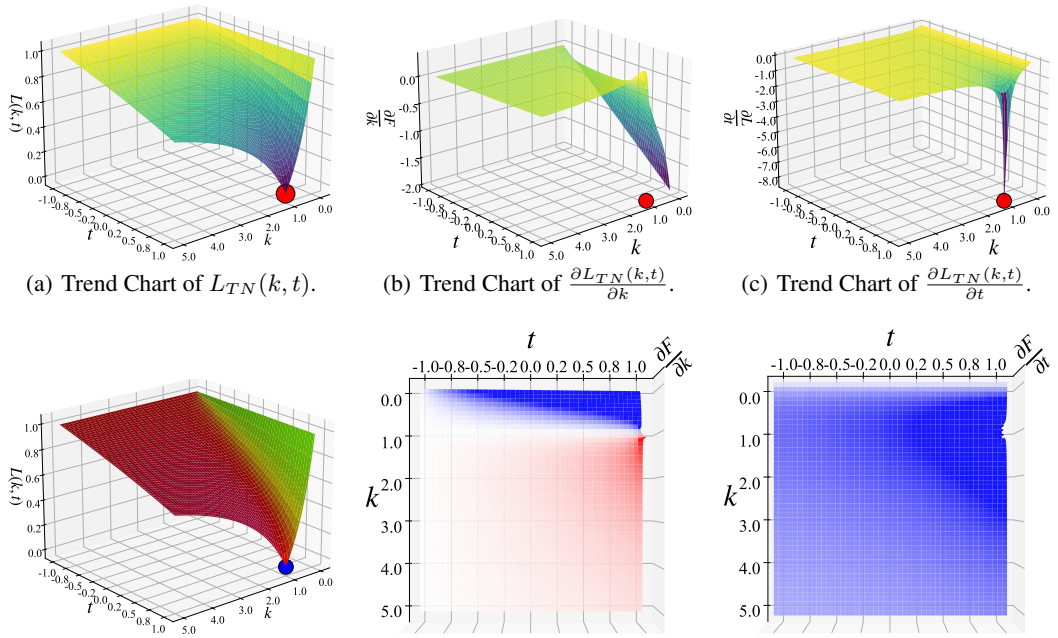

(a) Trend Chart of $L_{TN}(k,t)$. (b) Trend Chart of $\frac{\partial L_{TN}(k,t)}{\partial k}$. (c) Trend Chart of $\frac{\partial L_{TN}(k,t)}{\partial t}$.

(d) The direction and magnitude of the gradient of $L_{TN}(k,t)$. (e) View from above to observe the sign and magnitude of $\frac{\partial L_{TN}(k,t)}{\partial k}$. (f) View from above to observe the sign and magnitude of $\frac{\partial L_{TN}(k,t)}{\partial t}$.

Figure 2: The series of subfigures quantitatively analyzes L_{TN}. Subfigures (a)-(c) show trends of its primitive function and partial derivatives in t and k. Subfigure (d) overlays a gradient field on the function surface, red and green areas mark decreases driven by t and k, respectively, with darker shades indicating stronger influence. Subfigures (e) and (f) provide top-down views of sign distributions for $\frac{\partial L_{TN}}{\partial k}$ and $\frac{\partial L_{TN}}{\partial t}$, where blue/red denote negative/positive gradients, and darker colors show larger absolute values. For clarity, we mark the point (1, 1) in subfigures (a)-(d).

here, γ denotes the angle between tensors $\mathbf{h}_{qry}$ and $\mathbf{h}_{tgt}$. Since it is impossible to explicitly express the relationship between $\mathbf{h}_{qry}$ and $\mathbf{h}_{tgt}$ in any pair of positive samples, without loss of generality, we set $\|\mathbf{h}_{tgt}\| = k \cdot \|\mathbf{h}_{qry}\|$, $k \in (0, +\infty)$ and $t = \cos\gamma$, $t \in [-1, 1]$. Thus, Eq. 2 can be rewritten as a bivariate function of k and t, as shown in Eq. 3, which is visualized as Fig 2(a).

$$L_{TN}(k,t) = \frac{\sqrt{1+k^2-2\cdot kt}}{1+k}. \tag{3}$$

The ideal objective for L_{TN} is to simultaneously satisfy $\|\mathbf{h}_{qry}\| = \|\mathbf{h}_{tgt}\|$ and $\cos\gamma = 1$. This objective precisely corresponds to $k = 1$ and $t = 1$, ensuring perfect alignment between the two in both norm and direction. Although this configuration is intuitively desirable, existing works have not provided quantitative convergence proofs for this objective, nor has it systematically explored whether other local optima exist.

3.2 Proof of Monotonicity for Tensor Norm Constrained Loss Function L_{TN}

While TNCSE empirically shows that norm constraints on semantic representation tensors improve BERT-like models in semantic similarity tasks, it lacks theoretical justification. Here, we rigorously analyze why norm constraints benefit contrastive learning.

First, note that the Eq. 3 can be made a simple transformation. For any $k \in (0, +\infty)$ and $t \in [-1, 1]$, we have Ineq. 4:

$$0 \leq \frac{|k-1|}{k+1} = \frac{\sqrt{1+k^2-2\cdot k}}{1+k} \leq \frac{\sqrt{1+k^2-2\cdot kt}}{1+k} \leq \frac{\sqrt{1+k^2+2\cdot k}}{1+k} = 1, \tag{4}$$

which implies that $L_{\mathrm{TN}}(k,t) \geq 0$ throughout training, ensuring stable gradient updates. We expect k and t to converge to 1, driving h_{qry} and h_{tgt} to align in both norm and direction, which is consistent with our design motivation. To guarantee reliable optimization, however, we must formally

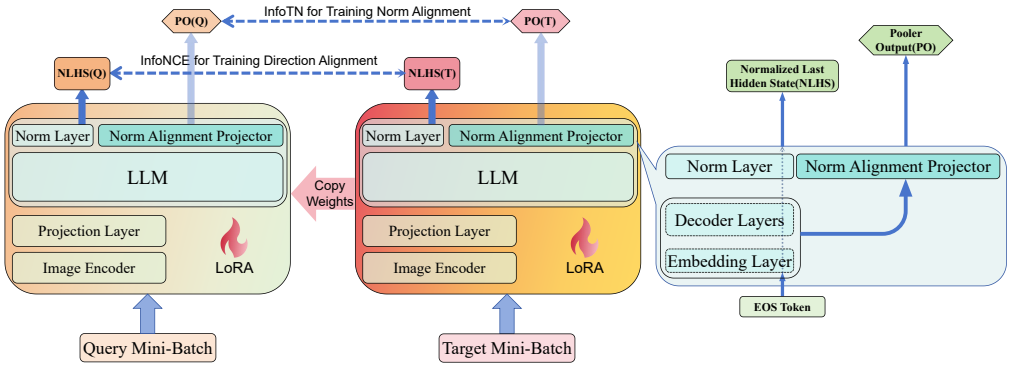

Figure 3: The architecture of our multimodal embedding representation framework, TNCME, which adds an FFN (Norm Alignment Projector, NAP) to a VLM. The hidden states are output by the LLM within the VLM, which passes through both a Norm Layer and the NAP. The resulting normalized last hidden state and projector output are trained by InfoNCE and InfoTN, respectively, to align the direction and norm of the multimodal query and target embedding representations.

show that k and t monotonically approach 1 without being trapped in spurious local optima. In the following, we prove that $L_{\mathrm{TN}}(k,t)$ is monotonic in both k and t.

First, we take the partial derivative of $L_{TN}(k,t)$ with the independent variable t to obtain Eq. 5:

$$\frac{\partial L_{TN}(k,t)}{\partial t} = -\frac{k}{(1+k)\cdot\sqrt{k^2-2kt+1}}, \tag{5}$$

It is observed that $\frac{\partial L_{TN}(k,t)}{\partial t} < 0$ holds throughout its domain[1]. Therefore, $L_{TN}(k,t)$ is monotonically decreasing in the t-direction, which means that for any $k > 0$ and $k \neq 1$, $L_{TN}(k,t)$ attains its minimum value at $t = 1$, and we visualize $\frac{\partial L_{TN}(k,t)}{\partial t}$ in Fig. 2(c) and 2(f). Then, we take the partial derivative of $L_{TN}(k,t)$ with respect to k, obtaining Eq. 6:

$$\frac{\partial L_{TN}(k,t)}{\partial k} = \frac{(k-1)\cdot(1+t)}{(1+k)^2\cdot\sqrt{k^2-2kt+1}}. \tag{6}$$

For any $t \in [-1,1)$, the behavior of $L_{\mathrm{TN}}(k,t)$ with respect to k is as follows: when $k \in [0,1)$, $\frac{\partial L_{\mathrm{TN}}(k,t)}{\partial k} < 0$, indicating that L_{TN} is decreasing in k; when $k > 1$, $\frac{\partial L_{\mathrm{TN}}(k,t)}{\partial k} > 0$, indicating that L_{TN} is increasing in k. Thus, $L_{\mathrm{TN}}(k,t)$ attains a local minimum at $k = 1$ along the k-direction. The behavior of $\frac{\partial L_{\mathrm{TN}}(k,t)}{\partial k}$ is visualized in Figs. 2(b) and 2(e).

In summary, we rigorously prove that $L_{\mathrm{TN}}(k,t)$ has a unique global minimum at $(k,t) = (1,1)$ within its domain, where $L_{\mathrm{TN}}(k,t) = 0$. This corresponds to perfect alignment between query and target in both norm and direction of their semantic representations, precisely the objective of our training framework. To further illustrate the optimization trajectory of $L_{\mathrm{TN}}(k,t)$, Fig. 2(d) visualizes the dominant influence of each variable during descent. The surface is color-mapped according to the gradient's direction and magnitude, highlighting the steepest descent directions across the domain. This reveals how k and t jointly govern the functional landscape and drive convergence toward the global minimum.

3.3 Model Structure Design

We employ a Qwen2VL model to encode queries and targets, utilizing the encoded last hidden states (LHS) for training. We observe that the LLM output representation tensor in the QwenVL series models will be normalized by RMSNorm(Zhang & Sennrich, 2019) to obtain the LHS. The LHS is clipped of norm features, retaining only directional features. VLM2Vec-V2 employs InfoNCE to set directional constraints on the LHS, and we need an FFN to reconstruct the norm features. Inspired by TNCSE, we observe that during generative tasks, QwenVL's LHS also passes through an FFN, referred to as the language model head (LM head). This head maps the LHS into a tensor of the

[1]We discuss in detail in Appendix A the effect of discontinuities that cause the denominator to become zero on monotonicity.

vocabulary size dimension, defined as logits, which are used for autoregressive tasks. Intuitively, one might consider using logits for tensor norm constraints. However, we find the logit distribution is excessively sparse and the output dimension of the LM head is prohibitively large, causing memory overflow even with LoRA(Hu et al., 2022) fine-tuning. Thus, we define a randomly initialized FFN after the LLM, as the **Norm Alignment Projector (NAP)**. Its purpose is to guide the model toward focusing on the semantic features required for retrieval tasks. The input and output dimensions of NAP align with the LHS, preventing memory overflow. We denote the features obtained by passing LHS through NAP as **Projector Output (PO)**, which captures the norm features of the representation. We employ PO in L_{TN} and LHS in InfoNCE, and train them jointly, as Fig. 3. NAP is used only in training, thus, the inference pipelines of TNCME and VLM2Vec-V2 are identical.

Given TNCSE's focus on pure text modalities, L_{TN} can be directly utilized for intuitive constraints. However, since TNCME focuses on multimodal data representation, ablation experiments reveal that directly applying L_{TN} results in convergence issues for the loss. Therefore, this subsection modifications to the L_{TN} is outlined in subsection 3.1, aiming to enhance its suitability for unsupervised contrastive learning of multimodal embeddings. First, we present the InfoNCE, in Eq. 7:

$$L_{InfoNCE} = -\log \frac{e^{sim\left(\mathbf{h}_{qry}, \mathbf{h}_{tgt^+}\right)/\tau}}{e^{sim\left(\mathbf{h}_{qry}, \mathbf{h}_{tgt^+}\right)/\tau} + \sum_{tgt^- \in \mathbb{N}} e^{sim\left(\mathbf{h}_{qry}, \mathbf{h}_{tgt^-}\right)/\tau}}, \tag{7}$$

where sim denotes cosine similarity, τ denotes the temperature coefficient, and $\mathbb{N}$ denotes the current mini-batch being trained. We observe that in the vast majority of cases, the cosine similarity distribution for multimodal positive and negative sample embeddings ranges from -0.01 to 1. According to Eq. 4, we have $0 \leq L(k,t) \leq 1$. Therefore, the range distribution of $L_{TN}(k,t)$ approximates the actual cosine similarity. Consequently, we define the norm similarity, as Eq. 8:

$$sim_{TN} = 1 - L_{TN}. \tag{8}$$

Since $L_{TN}(k,t)$ is expected to decrease during training while sim_{TN} increases, and $0 \leq sim_{TN} \leq 1$, we intuitively combine sim_{TN} and InfoNCE to propose the contrastive learning objective $Info_{TN}$ for multimodal embeddings, defined as Eq. 9:

$$L_{InfoTN} = -\log \frac{e^{\mathrm{sim}_{TN}\left(\mathbf{h}_{qry}, \mathbf{h}_{tgt^+}\right)/\tau_{TN}}}{e^{\mathrm{sim}_{TN}\left(\mathbf{h}_{qry}, \mathbf{h}_{tgt^+}\right)/\tau_{TN}} + \sum_{tgt^- \in \mathbb{N}} e^{\mathrm{sim}_{TN}\left(\mathbf{h}_{qry}, \mathbf{h}_{tgt^-}\right)/\tau_{TN}}}, \tag{9}$$

where τ_{TN} is also a temperature coefficient, independent of τ. This design effectively mitigates optimization obstacles caused by excessive differences in norm across different modalities, avoiding abrupt changes in the loss function triggered by the forced alignment of norm, and promotes stable convergence of the loss during training. We will visualize the changes in L_{InfoTN} and L_{TN} during training in ablation experiments to demonstrate the smoothness of InfoTN. Ultimately, we combine InfoTN and InfoNCE through joint training, defining the overall loss function as Eq. 10.

$$L = \lambda \cdot L_{InfoNCE} + (1-\lambda) \cdot L_{InfoTN}, \lambda \in (0,1)\,. \tag{10}$$

4 Experiments

4.1 Experimental Setup

We conduct experiments based on the VLM2Vec-V2 framework[2], which consists of three training tasks: Image-Text retrieval, VisDoc-Text retrieval, and Video-Text retrieval. All data are sourced from MMEB-train(Meng et al., 2025). To validate the method's generalization capability, we design three sets of progressive experiments: **(i)** Training solely on Image-Text data to evaluate image-text retrieval performance, and evaluating VisDoc-Text and Video-Text retrieval tasks under zero-shot conditions; **(ii)** Jointly training Image-Text and VisDoc-Text data, evaluating performance on both tasks, and conducting zero-shot evaluation on the Video-Text retrieval task; **(iii)** We use the full training set and then evaluate on three-class tasks[3]. Details of the datasets are listed in Appendix C. To thoroughly evaluate performance, we use multiple metrics,

[2] https://github.com/TIGER-AI-Lab/VLM2Vec

[3] Since the performance of reproduced VLM2Vec-V2 on the all training set shows a decline compared to the reported results, the issue remains unresolved as the manuscript submission; details are in Appendix B.

Table 1: We evaluate VLM2Vec-V2-Qwen2VL and TMCSE-Qwen2VL on three multimodal retrieval tasks: Image-Text (Im, 36 items), VisDoc-Text (Vd, 27 items), and Video-Text (Vi, 18 items). Results are averaged across subtasks and reported for eight metrics: Hit@k (H@k), NDCG-Linear@k (NL@k), NDCG-Exponential@k (NE@k), Precision@k (P@k), Recall@k (R@k), F1@k, MAP@k (MA@k), and MRR@k (MR@k). Top-1 scores are visually highlighted in . We also report the average improvement of TNCME over VLM2Vec-V2 separately, both the overall average (**Avg**) and the average @1 (**Avg @1**) derived from a total of 81 tasks.

Model	**VLM2Vec-V2**			**TNCME**			**VLM2Vec-V2**			**TNCME**			**VLM2Vec-V2**			**TNCME**		
Training	Image Only (5000 Steps)						Image and VisDoc (5000 Steps)						All Training-sets (2000 Steps)					
Metric	Im 36	Vd 27	Vi 18	Im 36	Vd 27	Vi 18	Im 36	Vd 27	Vi 18	Im 36	Vd 27	Vi 18	Im 36	Vd 27	Vi 18	Im 36	Vd 27	Vi 18
H@1	63.7	22.9	30.0	**64.9**	**24.5**	**31.4**	64.5	47.9	32.9	**65.3**	**49.1**	**33.0**	62.4	49.4	35.0	**62.8**	**50.3**	**35.2**
H@5	84.1	42.5	70.3	**85.0**	**43.0**	**72.1**	84.5	71.1	**73.2**	**84.9**	**72.2**	72.9	**83.9**	**73.0**	**74.1**	**83.9**	72.2	**74.1**
H@10	88.7	**52.1**	82.0	**89.5**	**52.1**	**83.1**	89.3	78.6	**83.6**	**89.5**	**80.1**	83.2	**88.7**	**79.6**	**84.3**	**88.7**	79.1	**84.3**
NL@1	63.7	21.6	30.0	**64.9**	**23.3**	**31.4**	64.5	46.2	32.9	**65.3**	**47.4**	**33.0**	62.4	47.8	35.0	**62.8**	**48.6**	**35.2**
NL@5	75.0	28.5	51.3	**76.1**	**29.7**	**52.8**	75.6	54.7	**54.2**	**76.2**	**56.0**	**54.2**	74.3	56.2	55.7	**74.5**	**56.3**	**55.9**
NL@10	76.5	30.9	55.1	**77.6**	**32.0**	**56.4**	77.1	56.7	57.5	**77.7**	**58.3**	**57.6**	75.9	57.9	59.0	**76.1**	**58.0**	**59.2**
NE@1	63.7	20.7	30.0	**64.9**	**22.5**	**31.4**	64.5	45.1	32.9	**65.3**	**46.2**	**33.0**	62.4	46.7	35.0	**62.8**	**47.4**	**35.2**
NE@5	75.0	28.0	51.3	**76.1**	**29.3**	**52.8**	75.6	54.0	**54.2**	**76.2**	**55.4**	**54.2**	74.3	55.6	55.7	**74.5**	**55.7**	**55.9**
NE@10	76.5	30.6	55.1	**77.6**	**31.7**	**56.4**	77.1	56.3	57.5	**77.7**	**57.9**	**57.6**	75.9	57.5	59.0	**76.1**	**57.6**	**59.2**
P@1	63.7	22.9	30.0	**64.9**	**24.5**	**31.4**	64.5	47.9	32.9	**65.3**	**49.1**	**33.0**	62.4	49.4	35.0	**62.8**	**50.3**	**35.2**
P@5	16.8	**11.9**	14.1	**17.0**	11.4	**14.5**	16.9	19.9	**14.7**	**17.0**	**20.5**	**14.7**	**16.8**	**20.5**	**14.9**	**16.8**	**20.5**	**14.9**
P@10	8.9	**8.8**	8.3	**9.0**	8.1	**8.4**	8.9	13.7	**8.4**	**9.0**	**14.1**	**8.4**	**8.9**	**13.6**	**8.5**	**8.9**	**13.6**	**8.5**
R@1	63.7	16.2	29.9	**64.9**	**18.3**	**31.3**	64.5	36.9	32.8	**65.3**	**38.3**	**32.9**	62.4	38.2	34.8	**62.8**	**38.6**	**35.1**
R@5	84.1	31.5	70.2	**85.0**	**32.9**	**72.0**	84.5	57.5	**73.2**	**84.9**	**58.5**	72.8	**83.9**	**59.1**	74.0	**83.9**	58.6	**74.1**
R@10	88.7	40.2	82.0	**89.5**	**40.9**	**83.1**	89.3	65.7	**83.6**	**89.5**	**67.4**	83.2	**88.7**	**66.6**	**84.3**	**88.7**	66.2	**84.3**
F@1	63.7	16.8	29.9	**64.9**	**18.9**	**31.3**	64.5	38.1	**32.9**	**65.3**	**39.5**	**32.9**	62.4	39.5	34.9	**62.8**	**40.0**	**35.1**
F@5	28.1	13.0	23.5	**28.3**	**13.2**	**24.1**	28.2	23.2	**24.5**	**28.3**	**23.8**	24.4	**28.0**	**23.9**	**24.8**	**28.0**	**23.9**	**24.8**
F@10	16.1	**10.7**	15.0	**16.3**	10.3	**15.2**	16.2	17.2	**15.3**	**16.3**	**17.7**	15.2	**16.1**	**17.3**	**15.4**	**16.1**	17.2	**15.4**
MA@1	63.7	22.9	30.0	**64.9**	**24.5**	**31.4**	64.5	47.9	32.9	**65.3**	**49.1**	**33.0**	62.4	49.4	35.0	**62.6**	**50.3**	**35.2**
MA@5	72.0	25.2	44.9	**73.1**	**26.7**	**46.4**	72.6	50.5	47.8	**73.2**	**52.1**	**48.0**	71.1	51.9	49.5	**71.3**	**52.2**	**49.9**
MA@10	72.6	25.6	46.5	**73.7**	**27.0**	**48.0**	73.2	50.6	49.2	**73.9**	**52.3**	**49.4**	71.7	51.7	50.9	**72.0**	**52.0**	**51.1**
MR@1	63.7	22.9	30.0	**64.9**	**24.5**	**31.4**	64.5	47.9	32.9	**65.3**	**49.1**	**33.0**	62.4	49.4	35.0	**62.8**	**50.2**	**35.2**
MR@5	72.0	29.9	45.0	**73.1**	**31.1**	**46.5**	72.6	56.7	47.9	**73.2**	**57.9**	**48.0**	71.1	58.5	49.6	**71.3**	**58.8**	**49.9**
MR@10	72.6	31.2	46.7	**73.7**	**32.3**	**48.0**	73.2	57.7	49.3	**73.9**	**59.0**	**49.4**	71.7	59.4	50.9	**72.0**	**59.7**	**51.2**
Avg	63.2	25.3	41.7	**64.1**	**26.4**	**42.9**	63.8	47.6	**44.1**	**64.3**	**48.8**	44.0	62.5	48.8	45.4	**62.7**	**49.0**	**45.6**
Avg @1		41.9		**43.3(+1.4%)**				50.9		**51.7(+0.8%)**				50.9		**51.4(+0.5%)**		

including Hit@1,5,10, NDCG-linear@1,5,10, NDCG-exponential@1,5,10, Precision@1,5,10, Recall@1,5,10, F1@1,5,10, MAP@1,5,10, and MRR@1,5,10, which capture retrieval quality from complementary perspectives as summarized in Appendix D[4]. Consistent with VLM2Vec-V2, we employ Qwen2-VL-2B as the backbone, and use the EOS token as the pooling method. All training is completed on 8 H100 GPUs with a total batch size set to 1024, a learning rate set to 5e-5, and a linear decay strategy is adopted. We adopt the LoRA fine-tuning strategy with rank set to 16 and scaling factor α set to 64. LoRA is implemented based on the PEFT(Mangrulkar et al., 2022) framework. In the first two experiments, which are conducted on subsets of the training data, we train for 5,000 steps. Due to computational resource constraints, we reduce the training steps to 2,000 when using the full training set[5]. The InfoNCE temperature τ is kept at its default value of 0.02 and λ is fixed at 0.5 across all configurations. To account for differences in training set distribution, we set τ_{TN} to 10^{-4} for the full training set, while the subset-based experiments use $\tau_{TN} = 0.05$.

4.2 Baseline Setting

VLM2Vec-V2 has demonstrated that VLM2Vec-V2-Qwen2VL-2B outperforms several recently open-sourced visual-language retrieval baselines across Image-Text, Video-Text, and Visdoc-Text tasks, such as ColPali-v1.3(Faysse et al., 2025a), GME-2B/7B(Zhang et al., 2024), LamRA-

[4]VLM2Vec-V2 employs Hit@1 as the metric for image-text retrieval tasks and VisDoc-text retrieval tasks, while NDCG@5 is used for video-text retrieval tasks. To comprehensively evaluate the model's performance across different tasks, we utilize all available evaluation metrics for a comprehensive evaluation.

[5]In VLM2Vec-V2, the authors mention training for either 2K or 5K steps; our settings are thus aligned with the original paper.

Qwen2/2.5-VL(Liu et al., 2025), VLM2Vec-2B/7B(Jiang et al., 2025), etc, as summerized in Appendix B. To demonstrate the superiority of our proposed method over VLM2Vec-V2, we retrain VLM2Vec-V2-Qwen2VL-2B as a baseline comparison using the same GPUs, official source code, and default parameters under three experimental conditions.

4.3 Results Analysis

We report the evaluation results of three experimental sets in Table 1. The experiments fully validate TNCME's significant advantage in enhancing Top-1 retrieval performance: across three distinct training set configurations, TNCME consistently outperforms the baseline model VLM2Vec-V2 on Top-1 metrics for all multimodal retrieval tasks (Image-Text, VisDoc-Text, Video-Text), demonstrating consistent and cross-modal generalization capabilities. Even when trained solely on image-text data, regardless of whether VisDoc or Video data is introduced, TNCME consistently maintains its lead, which demonstrates that the norm alignment mechanism exhibits strong robustness to training data composition, does not rely on specific modality distributions, and possesses broad applicability. Notably, even under the All-training-sets setting with only 2000 training steps, TNCME maintains its lead in Top-1 metrics, further demonstrating its stability. Although some metrics exhibit fluctuations at @5 and @10, which reflects a reasonable trade-off made to prioritize first-hit accuracy and does not undermine the model's core strengths.

5 Analysis and Ablation Study

5.1 Embedding Space Analysis

To more intuitively demonstrate the multimodal alignment between query and target embeddings, we employ t-SNE(Cieslak et al., 2020) visualization to analyze the embedding spaces of Qwen2VL, VLM2Vec-V2-Qwen2VL, and TNCME-Qwen2VL. Specifically, we randomly select 100 identical query-target sample pairs from the test set, reduce their high-dimensional embeddings to a two-dimensional space using t-SNE, and compute the Euclidean distance between each pair in this space. To enhance visualization, we connect queries and targets that are positive samples with each other using gray lines, as shown in Fig. 4. Visualization results indicate that the original Qwen2VL, untrained with contrastive learning, exhibits highly dispersed distributions of image and text embeddings, reflecting a lack of alignment between modalities. After introducing InfoNCE for directional alignment in VLM2Vec-V2-Qwen2VL, the distribution of positive pairs converges significantly, though some misalignment persists between modalities. TNCME-Qwen2VL achieves tighter positive sample clustering in the embedding space by jointly optimizing directional and norm alignment, significantly enhancing multimodal consistency. We quantitatively measure alignment performance by labeling the average Euclidean distance of the corresponding model in the 2D space on 100 sample pairs for each subgraph. Experimental, results show that compared to Qwen2VL and VLM2Vec-V2-Qwen2VL, TNCME-Qwen2VL reduces the average distance by 89.24% and 46.18%, respectively, fully validating the proposed method's significant advantage in enhancing cross-modal retrieval alignment capabilities for Qwen2VL.

Table 2: This table reports ablation results about whether to add FFN and whether to combine the training objective with InfoNCE, comparing with VLM2Vec-V2 and TNCME. All experiments are completed on image-text retrieval tasks.

Method	36 Avg Hit@1
VLM2Vec-V2	63.7
w/o. NAP	62.4
InfoNCE+L_{TN}	63.8
Our setting	**64.9**

5.2 Why Not Use L_{TN} Directly?

Fig. 4 illustrates a significant semantic gap between visual and textual representations in the backbone's initial state. Due to the batch size of 1024 during training, substantial discrepancies emerged in the norm of query and target representations, causing the L_{TN} loss to fluctuate violently during optimization and hindering convergence. This phenomenon doesn't occur in the pure text-modal TNCSE, indicating that the variance in representation norm distributions poses a challenge to training stability in multimodal scenarios; thus, the original method performs ineffectively. To address this, we construct InfoTN by combining L_{TN} with InfoNCE, which effectively mitigates the convergence issues caused by the variance in multimodal representation norm distributions, leading to a smoother and more stable loss curve. Fig. 5(b) compares the overall loss trends under both strate-

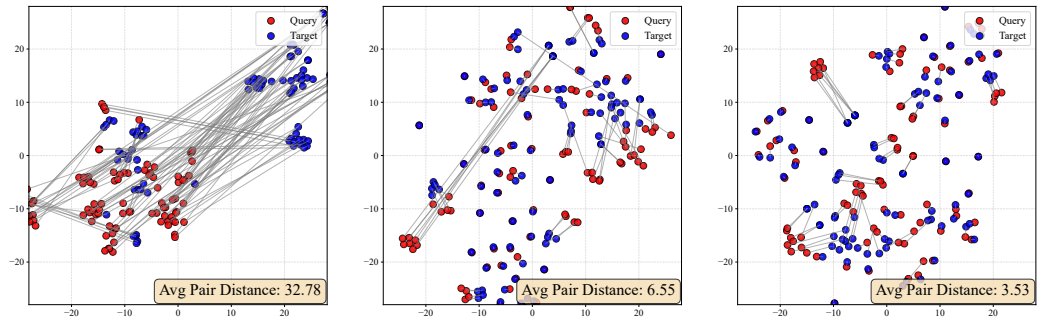

(a) Qwen2VL (b) VLM2Vec-V2-Qwen2VL (c) TNCME-Qwen2VL

Figure 4: This series of subfigures visualizes the embedding distributions of Qwen2VL, VLM2Vec-V2-Qwen2VL, and TNCME-Qwen2VL across 100 random sample pairs in a 2-dimensional space.

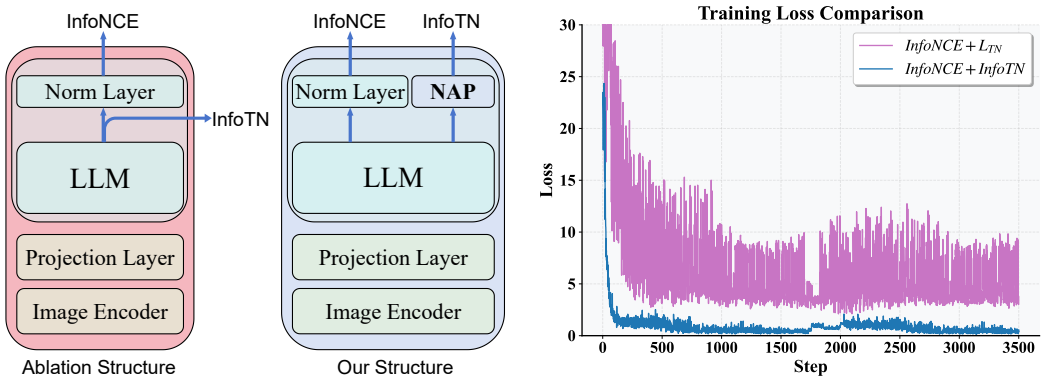

(a) (b)

Figure 5: Subfigure (a) illustrates the difference in training architecture with and without the NAP; Subfigure (b) reports that the loss fails to converge when training directly with L_{TN} in the image-text retrieval task.

gies, while Table 2 reports the final training performance results, confirming the proposed method's advantages in convergence and effectiveness.

5.3 Why Use an External FFN (NAP)?

The purpose of adding a feedforward neural network **NAP** in TNCME is to reconstruct the norm feature of the normalized last hidden state for joint training. Since the LLM output representation in Qwen2VL is not normalized and inherently possesses norm features, this representation passes through a final RMSNorm for normalization. The resulting LHS is then utilized for unsupervised contrastive learning training. To obtain the norm feature, an intuitive approach is to use the hidden state input to InfoTN without RMSNorm for norm alignment, while employing LHS for InfoNCE to achieve directional alignment, as shown in Fig. 5(a). However, this may be influenced by generative pretraining, introducing noise unrelated to norm alignment. Therefore, our approach involves initializing a decoupled FNN that maps raw hidden states to a new representation space, making their norm features more suitable for the InfoTN loss. We evaluate on 36 image-text retrieval tasks with consistent training hyperparameters, reporting results in Table 2.

6 Conclusion

In this paper, we first prove that norm alignment for embeddings is theoretically consistent with contrastive learning objectives. Building on this, we adapt the norm alignment objective for multimodal retrieval, aiming to boost Top-1 performance across metrics. Based on the VLM2Vec-V2 framework, we propose TNCME, a novel embedding approach trained with Qwen2VL-2B as the backbone. Evaluated on image-text, VisDoc-text, and video-text retrieval tasks, TNCME-Qwen2VL-2B consistently outperforms the replicated VLM2Vec-V2 baseline across all metrics. Ablation studies further validate the effectiveness of our method.

FUTURE WORKS

We adopt the latest Qwen2.5-VL(Bai et al., 2025) as both our backbone and the backbone for VLM2Vec-V2; however, experimental results show that it underperforms Qwen2-VL. This may stem from Qwen2.5VL employing an overly flexible dynamic pixel scaling strategy. Under large batch sizes, it necessitates compressing maximum pixel values to prevent out-of-memory errors. This may limit Qwen2.5VL's semantic expression capabilities, leading to suboptimal results. In the future, we will explore multimodal representation learning methods for VLM with flexible dynamic pixel scaling, exemplified by Qwen2.5-VL.

THE USAGE OF LLM

In this work, we use LLM to polish the mathematical derivation subsection in Appendix A and polish the Introduction and Method sections.

REPRODUCIBILITY STATEMENT

We have open-sourced the training and evaluation code for TNCME on an anonymous GitHub repository. Key hyperparameters are detailed in the Experimental Setup section of the paper. For further details, please refer to the training code.

ETHICS STATEMENT

This study does not involve any personal data, sensitive information, or high-risk application scenarios. No ethically controversial datasets or models were used. All experimental data are drawn from publicly available multimodal benchmark datasets, and the sole purpose of this research is to advance the development of multimodal representation learning. The study adheres strictly to data usage guidelines and does not involve any processing of the original data that could raise privacy or bias concerns. Therefore, we believe this work poses no significant ethical risks.

REFERENCES

Marah I Abdin, Sam Ade Jacobs, Ammar Ahmad Awan, Jyoti Aneja, Ahmed Awadallah, Hany Awadalla, Nguyen Bach, Amit Bahree, Arash Bakhtiari, Harkirat S. Behl, Alon Benhaim, Misha Bilenko, Johan Bjorck, Sébastien Bubeck, Martin Cai, Caio César Teodoro Mendes, Weizhu Chen, Vishrav Chaudhary, Parul Chopra, Allie Del Giorno, Gustavo de Rosa, Matthew Dixon, Ronen Eldan, Dan Iter, Amit Garg, Abhishek Goswami, Suriya Gunasekar, Emman Haider, Junheng Hao, Russell J. Hewett, Jamie Huynh, Mojan Javaheripi, Xin Jin, Piero Kauffmann, Nikos Karampatziakis, Dongwoo Kim, Mahoud Khademi, Lev Kurilenko, James R. Lee, Yin Tat Lee, Yuanzhi Li, Chen Liang, Weishung Liu, Eric Lin, Zeqi Lin, Piyush Madan, Arindam Mitra, Hardik Modi, Anh Nguyen, Brandon Norick, Barun Patra, Daniel Perez-Becker, Thomas Portet, Reid Pryzant, Heyang Qin, Marko Radmilac, Corby Rosset, Sambudha Roy, Olatunji Ruwase, Olli Saarikivi, Amin Saied, Adil Salim, Michael Santacroce, Shital Shah, Ning Shang, Hiteshi Sharma, Xia Song, Masahiro Tanaka, Xin Wang, Rachel Ward, Guanhua Wang, Philipp A. Witte, Michael Wyatt, Can Xu, Jiahang Xu, Sonali Yadav, Fan Yang, Ziyi Yang, Donghan Yu, Chengruidong Zhang, Cyril Zhang, Jianwen Zhang, Li Lyna Zhang, Yi Zhang, Yue Zhang, Yunan Zhang, and Xiren Zhou. Phi-3 technical report: A highly capable language model locally on your phone. *CoRR*, abs/2404.14219, 2024. doi: 10.48550/ARXIV.2404.14219. URL https://doi.org/10.48550/arXiv.2404.14219.

Jinze Bai, Shuai Bai, Yunfei Chu, Zeyu Cui, Kai Dang, Xiaodong Deng, Yang Fan, Wenbin Ge, Yu Han, Fei Huang, et al. Qwen technical report. *arXiv preprint arXiv:2309.16609*, 2023.

Shuai Bai, Keqin Chen, Xuejing Liu, Jialin Wang, Wenbin Ge, Sibo Song, Kai Dang, Peng Wang, Shijie Wang, Jun Tang, Humen Zhong, Yuanzhi Zhu, Ming-Hsuan Yang, Zhaohai Li, Jianqiang Wan, Pengfei Wang, Wei Ding, Zheren Fu, Yiheng Xu, Jiabo Ye, Xi Zhang, Tianbao Xie, Zesen Cheng, Hang Zhang, Zhibo Yang, Haiyang Xu, and Junyang Lin. Qwen2.5-vl technical report.

CoRR, abs/2502.13923, 2025. doi: 10.48550/ARXIV.2502.13923. URL https://doi.org/10.48550/arXiv.2502.13923.

Andrei Barbu, David Mayo, Julian Alverio, William Luo, Christopher Wang, Dan Gutfreund, Josh Tenenbaum, and Boris Katz. Objectnet: A large-scale bias-controlled dataset for pushing the limits of object recognition models. In Hanna M. Wallach, Hugo Larochelle, Alina Beygelzimer, Florence d'Alché-Buc, Emily B. Fox, and Roman Garnett (eds.), *Advances in Neural Information Processing Systems 32: Annual Conference on Neural Information Processing Systems 2019, NeurIPS 2019, December 8-14, 2019, Vancouver, BC, Canada*, pp. 9448–9458, 2019. URL https://proceedings.neurips.cc/paper/2019/hash/97af07a14cacba681feacf3012730892-Abstract.html.

João Carreira, Eric Noland, Chloe Hillier, and Andrew Zisserman. A short note on the kinetics-700 human action dataset. *CoRR*, abs/1907.06987, 2019. URL http://arxiv.org/abs/1907.06987.

Yingshan Chang, Guihong Cao, Mridu Narang, Jianfeng Gao, Hisami Suzuki, and Yonatan Bisk. Webqa: Multihop and multimodal QA. In *IEEE/CVF Conference on Computer Vision and Pattern Recognition, CVPR 2022, New Orleans, LA, USA, June 18-24, 2022*, pp. 16474–16483. IEEE, 2022. doi: 10.1109/CVPR52688.2022.01600. URL https://doi.org/10.1109/CVPR52688.2022.01600.

David L. Chen and William B. Dolan. Collecting highly parallel data for paraphrase evaluation. In Dekang Lin, Yuji Matsumoto, and Rada Mihalcea (eds.), *The 49th Annual Meeting of the Association for Computational Linguistics: Human Language Technologies, Proceedings of the Conference, 19-24 June, 2011, Portland, Oregon, USA*, pp. 190–200. The Association for Computer Linguistics, 2011. URL https://aclanthology.org/P11-1020/.

Matthew C. Cieslak, Ann M. Castelfranco, Vittoria Roncalli, Petra H. Lenz, and Daniel K. Hartline. t-distributed stochastic neighbor embedding (t-sne): A tool for eco-physiological transcriptomic analysis. *Marine Genomics*, 51:100723, 2020. ISSN 1874-7787. doi: https://doi.org/10.1016/j.margen.2019.100723. URL https://www.sciencedirect.com/science/article/pii/S1874778719301746.

Abhishek Das, Satwik Kottur, Khushi Gupta, Avi Singh, Deshraj Yadav, José M. F. Moura, Devi Parikh, and Dhruv Batra. Visual dialog. In *2017 IEEE Conference on Computer Vision and Pattern Recognition, CVPR 2017, Honolulu, HI, USA, July 21-26, 2017*, pp. 1080–1089. IEEE Computer Society, 2017. doi: 10.1109/CVPR.2017.121. URL https://doi.org/10.1109/CVPR.2017.121.

Jacob Devlin, Ming-Wei Chang, Kenton Lee, and Kristina Toutanova. BERT: pre-training of deep bidirectional transformers for language understanding. In Jill Burstein, Christy Doran, and Thamar Solorio (eds.), *Proceedings of the 2019 Conference of the North American Chapter of the Association for Computational Linguistics: Human Language Technologies, NAACL-HLT 2019, Minneapolis, MN, USA, June 2-7, 2019, Volume 1 (Long and Short Papers)*, pp. 4171–4186. Association for Computational Linguistics, 2019. doi: 10.18653/V1/N19-1423. URL https://doi.org/10.18653/v1/n19-1423.

Alon Diament, Maria Gorodetski, Adam Jankelow, Ayya Keshet, Tal Shor, Daphna Weissglas-Volkov, Hagai Rossman, and Eran Segal. A multimodal dataset of 21, 412 recorded nights for sleep and respiratory research. *CoRR*, abs/2311.08979, 2023. doi: 10.48550/ARXIV.2311.08979. URL https://doi.org/10.48550/arXiv.2311.08979.

Mark Everingham, Luc Van Gool, Christopher K. I. Williams, John M. Winn, and Andrew Zisserman. The pascal visual object classes (VOC) challenge. *Int. J. Comput. Vis.*, 88(2): 303–338, 2010. doi: 10.1007/S11263-009-0275-4. URL https://doi.org/10.1007/s11263-009-0275-4.

Manuel Faysse, Hugues Sibille, Tony Wu, Bilel Omrani, Gautier Viaud, Céline Hudelot, and Pierre Colombo. Colpali: Efficient document retrieval with vision language models. In *The Thirteenth International Conference on Learning Representations, ICLR 2025, Singapore, April 24-28, 2025*. OpenReview.net, 2025a. URL https://openreview.net/forum?id=ogjBpZ8uSi.

Manuel Faysse, Hugues Sibille, Tony Wu, Bilel Omrani, Gautier Viaud, Céline Hudelot, and Pierre Colombo. Colpali: Efficient document retrieval with vision language models. In *The Thirteenth International Conference on Learning Representations, ICLR 2025, Singapore, April 24-28, 2025*. OpenReview.net, 2025b. URL https://openreview.net/forum?id=ogjBpZ8uSi.

Chaoyou Fu, Yuhan Dai, Yongdong Luo, Lei Li, Shuhuai Ren, Renrui Zhang, Zihan Wang, Chenyu Zhou, Yunhang Shen, Mengdan Zhang, Peixian Chen, Yanwei Li, Shaohui Lin, Sirui Zhao, Ke Li, Tong Xu, Xiawu Zheng, Enhong Chen, Caifeng Shan, Ran He, and Xing Sun. Video-mme: The first-ever comprehensive evaluation benchmark of multi-modal llms in video analysis. In *IEEE/CVF Conference on Computer Vision and Pattern Recognition, CVPR 2025, Nashville, TN, USA, June 11-15, 2025*, pp. 24108–24118. Computer Vision Foundation / IEEE, 2025. doi: 10.1109/CVPR52734.2025.02245. URL https://openaccess.thecvf.com/content/CVPR2025/html/Fu_Video-MME_The_First-Ever_Comprehensive_Evaluation_Benchmark_of_Multi-modal_LLMs_in_CVPR_2025_paper.html.

Jiyang Gao, Chen Sun, Zhenheng Yang, and Ram Nevatia. TALL: temporal activity localization via language query. In *IEEE International Conference on Computer Vision, ICCV 2017, Venice, Italy, October 22-29, 2017*, pp. 5277–5285. IEEE Computer Society, 2017. doi: 10.1109/ICCV.2017.563. URL https://doi.org/10.1109/ICCV.2017.563.

Tianyu Gao, Xingcheng Yao, and Danqi Chen. Simcse: Simple contrastive learning of sentence embeddings. In Marie-Francine Moens, Xuanjing Huang, Lucia Specia, and Scott Wen-tau Yih (eds.), *Proceedings of the 2021 Conference on Empirical Methods in Natural Language Processing, EMNLP 2021, Virtual Event / Punta Cana, Dominican Republic, 7-11 November, 2021*, pp. 6894–6910. Association for Computational Linguistics, 2021. doi: 10.18653/V1/2021.EMNLP-MAIN.552. URL https://doi.org/10.18653/v1/2021.emnlp-main.552.

Raghav Goyal, Samira Ebrahimi Kahou, Vincent Michalski, Joanna Materzynska, Susanne Westphal, Heuna Kim, Valentin Haenel, Ingo Fründ, Peter Yianilos, Moritz Mueller-Freitag, Florian Hoppe, Christian Thurau, Ingo Bax, and Roland Memisevic. The "something something" video database for learning and evaluating visual common sense. In *IEEE International Conference on Computer Vision, ICCV 2017, Venice, Italy, October 22-29, 2017*, pp. 5843–5851. IEEE Computer Society, 2017. doi: 10.1109/ICCV.2017.622. URL https://doi.org/10.1109/ICCV.2017.622.

Danna Gurari, Qing Li, Abigale J. Stangl, Anhong Guo, Chi Lin, Kristen Grauman, Jiebo Luo, and Jeffrey P. Bigham. Vizwiz grand challenge: Answering visual questions from blind people. In *2018 IEEE Conference on Computer Vision and Pattern Recognition, CVPR 2018, Salt Lake City, UT, USA, June 18-22, 2018*, pp. 3608–3617. Computer Vision Foundation / IEEE Computer Society, 2018. doi: 10.1109/CVPR.2018.00380. URL http://openaccess.thecvf.com/content_cvpr_2018/html/Gurari_VizWiz_Grand_Challenge_CVPR_2018_paper.html.

Lisa Anne Hendricks, Oliver Wang, Eli Shechtman, Josef Sivic, Trevor Darrell, and Bryan C. Russell. Localizing moments in video with natural language. In *IEEE International Conference on Computer Vision, ICCV 2017, Venice, Italy, October 22-29, 2017*, pp. 5804–5813. IEEE Computer Society, 2017. doi: 10.1109/ICCV.2017.618. URL https://doi.org/10.1109/ICCV.2017.618.

Dan Hendrycks, Kevin Zhao, Steven Basart, Jacob Steinhardt, and Dawn Song. Natural adversarial examples. *CoRR*, abs/1907.07174, 2019. URL http://arxiv.org/abs/1907.07174.

Dan Hendrycks, Steven Basart, Norman Mu, Saurav Kadavath, Frank Wang, Evan Dorundo, Rahul Desai, Tyler Zhu, Samyak Parajuli, Mike Guo, Dawn Song, Jacob Steinhardt, and Justin Gilmer. The many faces of robustness: A critical analysis of out-of-distribution generalization. In *2021 IEEE/CVF International Conference on Computer Vision, ICCV 2021, Montreal, QC, Canada, October 10-17, 2021*, pp. 8320–8329. IEEE, 2021. doi: 10.1109/ICCV48922.2021.00823. URL https://doi.org/10.1109/ICCV48922.2021.00823.

Edward J. Hu, Yelong Shen, Phillip Wallis, Zeyuan Allen-Zhu, Yuanzhi Li, Shean Wang, Lu Wang, and Weizhu Chen. Lora: Low-rank adaptation of large language models. In *The Tenth International Conference on Learning Representations, ICLR 2022, Virtual Event, April 25-29, 2022*. OpenReview.net, 2022. URL https://openreview.net/forum?id=nZeVKeeFYf9.

Hexiang Hu, Yi Luan, Yang Chen, Urvashi Khandelwal, Mandar Joshi, Kenton Lee, Kristina Toutanova, and Ming-Wei Chang. Open-domain visual entity recognition: Towards recognizing millions of wikipedia entities. In *IEEE/CVF International Conference on Computer Vision, ICCV 2023, Paris, France, October 1-6, 2023*, pp. 12031–12041. IEEE, 2023. doi: 10.1109/ICCV51070.2023.01108. URL https://doi.org/10.1109/ICCV51070.2023.01108.

Drew A. Hudson and Christopher D. Manning. GQA: A new dataset for real-world visual reasoning and compositional question answering. In *IEEE Conference on Computer Vision and Pattern Recognition, CVPR 2019, Long Beach, CA, USA, June 16-20, 2019*, pp. 6700–6709. Computer Vision Foundation / IEEE, 2019. doi: 10.1109/CVPR.2019.00686. URL http://openaccess.thecvf.com/content_CVPR_2019/html/Hudson_GQA_A_New_Dataset_for_Real-World_Visual_Reasoning_and_Compositional_CVPR_2019_paper.html.

Ziyan Jiang, Rui Meng, Xinyi Yang, Semih Yavuz, Yingbo Zhou, and Wenhu Chen. Vlm2vec: Training vision-language models for massive multimodal embedding tasks. In *The Thirteenth International Conference on Learning Representations, ICLR 2025, Singapore, April 24-28, 2025*. OpenReview.net, 2025. URL https://openreview.net/forum?id=TE0KOzWYAF.

Sahar Kazemzadeh, Vicente Ordonez, Mark Matten, and Tamara L. Berg. Referitgame: Referring to objects in photographs of natural scenes. In Alessandro Moschitti, Bo Pang, and Walter Daelemans (eds.), *Proceedings of the 2014 Conference on Empirical Methods in Natural Language Processing, EMNLP 2014, October 25-29, 2014, Doha, Qatar, A meeting of SIGDAT, a Special Interest Group of the ACL*, pp. 787–798. ACL, 2014. doi: 10.3115/V1/D14-1086. URL https://doi.org/10.3115/v1/d14-1086.

Douwe Kiela, Hamed Firooz, Aravind Mohan, Vedanuj Goswami, Amanpreet Singh, Pratik Ringshia, and Davide Testuggine. The hateful memes challenge: Detecting hate speech in multimodal memes. In Hugo Larochelle, Marc'Aurelio Ranzato, Raia Hadsell, Maria-Florina Balcan, and Hsuan-Tien Lin (eds.), *Advances in Neural Information Processing Systems 33: Annual Conference on Neural Information Processing Systems 2020, NeurIPS 2020, December 6-12, 2020, virtual*, 2020. URL https://proceedings.neurips.cc/paper/2020/hash/1b84c4cee2b8b3d823b30e2d604b1878-Abstract.html.

Hilde Kuehne, Ali Bilgin Arslan, and Thomas Serre. The language of actions: Recovering the syntax and semantics of goal-directed human activities. In *2014 IEEE Conference on Computer Vision and Pattern Recognition, CVPR 2014, Columbus, OH, USA, June 23-28, 2014*, pp. 780–787. IEEE Computer Society, 2014. doi: 10.1109/CVPR.2014.105. URL https://doi.org/10.1109/CVPR.2014.105.

Hildegard Kuehne, Hueihan Jhuang, Estíbaliz Garrote, Tomaso A. Poggio, and Thomas Serre. HMDB: A large video database for human motion recognition. In Dimitris N. Metaxas, Long Quan, Alberto Sanfeliu, and Luc Van Gool (eds.), *IEEE International Conference on Computer Vision, ICCV 2011, Barcelona, Spain, November 6-13, 2011*, pp. 2556–2563. IEEE Computer Society, 2011. doi: 10.1109/ICCV.2011.6126543. URL https://doi.org/10.1109/ICCV.2011.6126543.

Jie Lei, Tamara L. Berg, and Mohit Bansal. Qvhighlights: Detecting moments and highlights in videos via natural language queries. *CoRR*, abs/2107.09609, 2021. URL https://arxiv.org/abs/2107.09609.

Junnan Li, Dongxu Li, Caiming Xiong, and Steven C. H. Hoi. BLIP: bootstrapping language-image pre-training for unified vision-language understanding and generation. In Kamalika Chaudhuri, Stefanie Jegelka, Le Song, Csaba Szepesvári, Gang Niu, and Sivan Sabato (eds.), *International Conference on Machine Learning, ICML 2022, 17-23 July 2022, Baltimore, Maryland, USA*,

volume 162 of *Proceedings of Machine Learning Research*, pp. 12888–12900. PMLR, 2022. URL https://proceedings.mlr.press/v162/li22n.html.

Junnan Li, Dongxu Li, Silvio Savarese, and Steven C. H. Hoi. BLIP-2: bootstrapping language-image pre-training with frozen image encoders and large language models. In Andreas Krause, Emma Brunskill, Kyunghyun Cho, Barbara Engelhardt, Sivan Sabato, and Jonathan Scarlett (eds.), *International Conference on Machine Learning, ICML 2023, 23-29 July 2023, Honolulu, Hawaii, USA*, volume 202 of *Proceedings of Machine Learning Research*, pp. 19730–19742. PMLR, 2023. URL https://proceedings.mlr.press/v202/li23q.html.

Kunchang Li, Yali Wang, Yinan He, Yizhuo Li, Yi Wang, Yi Liu, Zun Wang, Jilan Xu, Guo Chen, Ping Lou, Limin Wang, and Yu Qiao. Mvbench: A comprehensive multi-modal video understanding benchmark. In *IEEE/CVF Conference on Computer Vision and Pattern Recognition, CVPR 2024, Seattle, WA, USA, June 16-22, 2024*, pp. 22195–22206. IEEE, 2024. doi: 10.1109/CVPR52733.2024.02095. URL https://doi.org/10.1109/CVPR52733.2024.02095.

Tsung-Yi Lin, Michael Maire, Serge J. Belongie, James Hays, Pietro Perona, Deva Ramanan, Piotr Dollár, and C. Lawrence Zitnick. Microsoft COCO: common objects in context. In David J. Fleet, Tomás Pajdla, Bernt Schiele, and Tinne Tuytelaars (eds.), *Computer Vision - ECCV 2014 - 13th European Conference, Zurich, Switzerland, September 6-12, 2014, Proceedings, Part V*, volume 8693 of *Lecture Notes in Computer Science*, pp. 740–755. Springer, 2014. doi: 10.1007/978-3-319-10602-1_48. URL https://doi.org/10.1007/978-3-319-10602-1_48.

Fuxiao Liu, Yinghan Wang, Tianlu Wang, and Vicente Ordonez. Visual news: Benchmark and challenges in news image captioning. In Marie-Francine Moens, Xuanjing Huang, Lucia Specia, and Scott Wen-tau Yih (eds.), *Proceedings of the 2021 Conference on Empirical Methods in Natural Language Processing, EMNLP 2021, Virtual Event / Punta Cana, Dominican Republic, 7-11 November, 2021*, pp. 6761–6771. Association for Computational Linguistics, 2021a. doi: 10.18653/V1/2021.EMNLP-MAIN.542. URL https://doi.org/10.18653/v1/2021.emnlp-main.542.

Haotian Liu, Chunyuan Li, Qingyang Wu, and Yong Jae Lee. Visual instruction tuning. In Alice Oh, Tristan Naumann, Amir Globerson, Kate Saenko, Moritz Hardt, and Sergey Levine (eds.), *Advances in Neural Information Processing Systems 36: Annual Conference on Neural Information Processing Systems 2023, NeurIPS 2023, New Orleans, LA, USA, December 10 - 16, 2023*, 2023a. URL http://papers.nips.cc/paper_files/paper/2023/hash/6dcf277ea32ce3288914faf369fe6de0-Abstract-Conference.html.

Haotian Liu, Chunyuan Li, Yuheng Li, and Yong Jae Lee. Improved baselines with visual instruction tuning. In *IEEE/CVF Conference on Computer Vision and Pattern Recognition, CVPR 2024, Seattle, WA, USA, June 16-22, 2024*, pp. 26286–26296. IEEE, 2024a. doi: 10.1109/CVPR52733.2024.02484. URL https://doi.org/10.1109/CVPR52733.2024.02484.

Haotian Liu, Chunyuan Li, Yuheng Li, Bo Li, Yuanhan Zhang, Sheng Shen, and Yong Jae Lee. Llava-next: Improved reasoning, ocr, and world knowledge, January 2024b. URL https://llava-vl.github.io/blog/2024-01-30-llava-next/.

Siqi Liu, Weixi Feng, Tsu-Jui Fu, Wenhu Chen, and William Wang. EDIS: entity-driven image search over multimodal web content. In Houda Bouamor, Juan Pino, and Kalika Bali (eds.), *Proceedings of the 2023 Conference on Empirical Methods in Natural Language Processing, EMNLP 2023, Singapore, December 6-10, 2023*, pp. 4877–4894. Association for Computational Linguistics, 2023b. doi: 10.18653/V1/2023.EMNLP-MAIN.297. URL https://doi.org/10.18653/v1/2023.emnlp-main.297.

Yikun Liu, Yajie Zhang, Jiayin Cai, Xiaolong Jiang, Yao Hu, Jiangchao Yao, Yanfeng Wang, and Weidi Xie. Lamra: Large multimodal model as your advanced retrieval assistant. In *IEEE/CVF Conference on Computer Vision and Pattern Recognition, CVPR 2025, Nashville, TN, USA, June 11-15, 2025*, pp. 4015–4025. Computer Vision Foundation / IEEE, 2025. doi: 10.1109/CVPR52734.2025.00380. URL https://openaccess.thecvf.com/

content/CVPR2025/html/Liu_LamRA_Large_Multimodal_Model_as_Your_Advanced_Retrieval_Assistant_CVPR_2025_paper.html.

Yinhan Liu, Myle Ott, Naman Goyal, Jingfei Du, Mandar Joshi, Danqi Chen, Omer Levy, Mike Lewis, Luke Zettlemoyer, and Veselin Stoyanov. Roberta: A robustly optimized BERT pretraining approach. *CoRR*, abs/1907.11692, 2019. URL http://arxiv.org/abs/1907.11692.

Zheyuan Liu, Cristian Rodriguez Opazo, Damien Teney, and Stephen Gould. Image retrieval on real-life images with pre-trained vision-and-language models. In *2021 IEEE/CVF International Conference on Computer Vision, ICCV 2021, Montreal, QC, Canada, October 10-17, 2021*, pp. 2105–2114. IEEE, 2021b. doi: 10.1109/ICCV48922.2021.00213. URL https://doi.org/10.1109/ICCV48922.2021.00213.

Pan Lu, Swaroop Mishra, Tanglin Xia, Liang Qiu, Kai-Wei Chang, Song-Chun Zhu, Oyvind Tafjord, Peter Clark, and Ashwin Kalyan. Learn to explain: Multimodal reasoning via thought chains for science question answering. In Sanmi Koyejo, S. Mohamed, A. Agarwal, Danielle Belgrave, K. Cho, and A. Oh (eds.), *Advances in Neural Information Processing Systems 35: Annual Conference on Neural Information Processing Systems 2022, NeurIPS 2022, New Orleans, LA, USA, November 28 - December 9, 2022*, 2022. URL http://papers.nips.cc/paper_files/paper/2022/hash/11332b6b6cf4485b84afadb1352d3a9a-Abstract-Conference.html.

Xueguang Ma, Sheng-Chieh Lin, Minghan Li, Wenhu Chen, and Jimmy Lin. Unifying multimodal retrieval via document screenshot embedding. In Yaser Al-Onaizan, Mohit Bansal, and Yun-Nung Chen (eds.), *Proceedings of the 2024 Conference on Empirical Methods in Natural Language Processing, EMNLP 2024, Miami, FL, USA, November 12-16, 2024*, pp. 6492–6505. Association for Computational Linguistics, 2024a. doi: 10.18653/V1/2024.EMNLP-MAIN.373. URL https://doi.org/10.18653/v1/2024.emnlp-main.373.

Yubo Ma, Yuhang Zang, Liangyu Chen, Meiqi Chen, Yizhu Jiao, Xinze Li, Xinyuan Lu, Ziyu Liu, Yan Ma, Xiaoyi Dong, Pan Zhang, Liangming Pan, Yu-Gang Jiang, Jiaqi Wang, Yixin Cao, and Aixin Sun. MMLONGBENCH-DOC: benchmarking long-context document understanding with visualizations. In Amir Globersons, Lester Mackey, Danielle Belgrave, Angela Fan, Ulrich Paquet, Jakub M. Tomczak, and Cheng Zhang (eds.), *Advances in Neural Information Processing Systems 38: Annual Conference on Neural Information Processing Systems 2024, NeurIPS 2024, Vancouver, BC, Canada, December 10 - 15, 2024*, 2024b. URL http://papers.nips.cc/paper_files/paper/2024/hash/ae0e43289bffea0c1fa34633fc608e92-Abstract-Datasets_and_Benchmarks_Track.html.

Quentin Macé, António Loison, and Manuel Faysse. Vidore benchmark V2: raising the bar for visual retrieval. *CoRR*, abs/2505.17166, 2025. doi: 10.48550/ARXIV.2505.17166. URL https://doi.org/10.48550/arXiv.2505.17166.

Karttikeya Mangalam, Raiymbek Akshulakov, and Jitendra Malik. Egoschema: A diagnostic benchmark for very long-form video language understanding. In Alice Oh, Tristan Naumann, Amir Globerson, Kate Saenko, Moritz Hardt, and Sergey Levine (eds.), *Advances in Neural Information Processing Systems 36: Annual Conference on Neural Information Processing Systems 2023, NeurIPS 2023, New Orleans, LA, USA, December 10 - 16, 2023*, 2023. URL http://papers.nips.cc/paper_files/paper/2023/hash/90ce332aff156b910b002ce4e6880dec-Abstract-Datasets_and_Benchmarks.html.

Sourab Mangrulkar, Sylvain Gugger, Lysandre Debut, Younes Belkada, Sayak Paul, and Benjamin Bossan. PEFT: State-of-the-art parameter-efficient fine-tuning methods. https://github.com/huggingface/peft, 2022.

Kenneth Marino, Mohammad Rastegari, Ali Farhadi, and Roozbeh Mottaghi. OK-VQA: A visual question answering benchmark requiring external knowledge. In *IEEE Conference on Computer Vision and Pattern Recognition, CVPR 2019, Long Beach, CA, USA, June 16-20, 2019*, pp. 3195–3204. Computer Vision Foundation / IEEE, 2019. doi: 10.1109/CVPR.2019.00331. URL http://openaccess.thecvf.com/content_CVPR_2019/html/Marino_

OK-VQA_A_Visual_Question_Answering_Benchmark_Requiring_External_Knowledge_CVPR_2019_paper.html.

Ahmed Masry, Do Xuan Long, Jia Qing Tan, Shafiq R. Joty, and Enamul Hoque. Chartqa: A benchmark for question answering about charts with visual and logical reasoning. In Smaranda Muresan, Preslav Nakov, and Aline Villavicencio (eds.), *Findings of the Association for Computational Linguistics: ACL 2022, Dublin, Ireland, May 22-27, 2022*, pp. 2263–2279. Association for Computational Linguistics, 2022. doi: 10.18653/V1/2022.FINDINGS-ACL.177. URL https://doi.org/10.18653/v1/2022.findings-acl.177.

Minesh Mathew, Dimosthenis Karatzas, and C. V. Jawahar. Docvqa: A dataset for VQA on document images. In *IEEE Winter Conference on Applications of Computer Vision, WACV 2021, Waikoloa, HI, USA, January 3-8, 2021*, pp. 2199–2208. IEEE, 2021. doi: 10.1109/WACV48630.2021.00225. URL https://doi.org/10.1109/WACV48630.2021.00225.

Minesh Mathew, Viraj Bagal, Rubèn Tito, Dimosthenis Karatzas, Ernest Valveny, and C. V. Jawahar. Infographicvqa. In *IEEE/CVF Winter Conference on Applications of Computer Vision, WACV 2022, Waikoloa, HI, USA, January 3-8, 2022*, pp. 2582–2591. IEEE, 2022. doi: 10.1109/WACV51458.2022.00264. URL https://doi.org/10.1109/WACV51458.2022.00264.

Rui Meng, Ziyan Jiang, Ye Liu, Mingyi Su, Xinyi Yang, Yuepeng Fu, Can Qin, Zeyuan Chen, Ran Xu, Caiming Xiong, Yingbo Zhou, Wenhu Chen, and Semih Yavuz. Vlm2vec-v2: Advancing multimodal embedding for videos, images, and visual documents. *CoRR*, abs/2507.04590, 2025. doi: 10.48550/ARXIV.2507.04590. URL https://doi.org/10.48550/arXiv.2507.04590.

Alec Radford, Jong Wook Kim, Chris Hallacy, Aditya Ramesh, Gabriel Goh, Sandhini Agarwal, Girish Sastry, Amanda Askell, Pamela Mishkin, Jack Clark, Gretchen Krueger, and Ilya Sutskever. Learning transferable visual models from natural language supervision. In Marina Meila and Tong Zhang (eds.), *Proceedings of the 38th International Conference on Machine Learning, ICML 2021, 18-24 July 2021, Virtual Event*, volume 139 of *Proceedings of Machine Learning Research*, pp. 8748–8763. PMLR, 2021a. URL http://proceedings.mlr.press/v139/radford21a.html.

Alec Radford, Jong Wook Kim, Chris Hallacy, Aditya Ramesh, Gabriel Goh, Sandhini Agarwal, Girish Sastry, Amanda Askell, Pamela Mishkin, Jack Clark, Gretchen Krueger, and Ilya Sutskever. Learning transferable visual models from natural language supervision. In Marina Meila and Tong Zhang (eds.), *Proceedings of the 38th International Conference on Machine Learning, ICML 2021, 18-24 July 2021, Virtual Event*, volume 139 of *Proceedings of Machine Learning Research*, pp. 8748–8763. PMLR, 2021b. URL http://proceedings.mlr.press/v139/radford21a.html.

Nils Reimers and Iryna Gurevych. Sentence-bert: Sentence embeddings using siamese bert-networks. In Kentaro Inui, Jing Jiang, Vincent Ng, and Xiaojun Wan (eds.), *Proceedings of the 2019 Conference on Empirical Methods in Natural Language Processing and the 9th International Joint Conference on Natural Language Processing, EMNLP-IJCNLP 2019, Hong Kong, China, November 3-7, 2019*, pp. 3980–3990. Association for Computational Linguistics, 2019. doi: 10.18653/V1/D19-1410. URL https://doi.org/10.18653/v1/D19-1410.

Olga Russakovsky, Jia Deng, Hao Su, Jonathan Krause, Sanjeev Satheesh, Sean Ma, Zhiheng Huang, Andrej Karpathy, Aditya Khosla, Michael S. Bernstein, Alexander C. Berg, and Li Fei-Fei. Imagenet large scale visual recognition challenge. *Int. J. Comput. Vis.*, 115(3): 211–252, 2015. doi: 10.1007/S11263-015-0816-Y. URL https://doi.org/10.1007/s11263-015-0816-y.

Dustin Schwenk, Apoorv Khandelwal, Christopher Clark, Kenneth Marino, and Roozbeh Mottaghi. A-OKVQA: A benchmark for visual question answering using world knowledge. In Shai Avidan, Gabriel J. Brostow, Moustapha Cissé, Giovanni Maria Farinella, and Tal Hassner (eds.), *Computer Vision - ECCV 2022 - 17th European Conference, Tel Aviv, Israel, October 23-27, 2022, Proceedings, Part VIII*, volume 13668 of *Lecture Notes in Computer Science*, pp. 146–162. Springer, 2022. doi: 10.1007/978-3-031-20074-8_9. URL https://doi.org/10.1007/978-3-031-20074-8_9.

Amanpreet Singh, Vivek Natarajan, Meet Shah, Yu Jiang, Xinlei Chen, Dhruv Batra, Devi Parikh, and Marcus Rohrbach. Towards VQA models that can read. In *IEEE Conference on Computer Vision and Pattern Recognition, CVPR 2019, Long Beach, CA, USA, June 16-20, 2019*, pp. 8317–8326. Computer Vision Foundation / IEEE, 2019. doi: 10.1109/CVPR.2019.00851. URL http://openaccess.thecvf.com/content_CVPR_2019/html/Singh_Towards_VQA_Models_That_Can_Read_CVPR_2019_paper.html.

Khurram Soomro, Amir Roshan Zamir, and Mubarak Shah. UCF101: A dataset of 101 human actions classes from videos in the wild. *CoRR*, abs/1212.0402, 2012. URL http://arxiv.org/abs/1212.0402.

Aäron van den Oord, Yazhe Li, and Oriol Vinyals. Representation learning with contrastive predictive coding. *CoRR*, abs/1807.03748, 2018. URL http://arxiv.org/abs/1807.03748.

Qiuchen Wang, Ruixue Ding, Zehui Chen, Weiqi Wu, Shihang Wang, Pengjun Xie, and Feng Zhao. Vidorag: Visual document retrieval-augmented generation via dynamic iterative reasoning agents. *CoRR*, abs/2502.18017, 2025a. doi: 10.48550/ARXIV.2502.18017. URL https://doi.org/10.48550/arXiv.2502.18017.

Weizhi Wang, Yu Tian, Linjie Yang, Heng Wang, and Xifeng Yan. Open-qwen2vl: Compute-efficient pre-training of fully-open multimodal llms on academic resources. *CoRR*, abs/2504.00595, 2025b. doi: 10.48550/ARXIV.2504.00595. URL https://doi.org/10.48550/arXiv.2504.00595.

Xin Wang, Jiawei Wu, Jun-Kun Chen, Lei Li, Yuan-Fang Wang, and William Yang Wang. Vatex: A large-scale, high-quality multilingual dataset for video-and-language research. In *2019 IEEE/CVF International Conference on Computer Vision, ICCV 2019, Seoul, Korea (South), October 27 - November 2, 2019*, pp. 4580–4590. IEEE, 2019. doi: 10.1109/ICCV.2019.00468. URL https://doi.org/10.1109/ICCV.2019.00468.

Zhen Wang, Xu Shan, Xiangxie Zhang, and Jie Yang. N24news: A new dataset for multimodal news classification. In Nicoletta Calzolari, Frédéric Béchet, Philippe Blache, Khalid Choukri, Christopher Cieri, Thierry Declerck, Sara Goggi, Hitoshi Isahara, Bente Maegaard, Joseph Mariani, Hélène Mazo, Jan Odijk, and Stelios Piperidis (eds.), *Proceedings of the Thirteenth Language Resources and Evaluation Conference, LREC 2022, Marseille, France, 20-25 June 2022*, pp. 6768–6775. European Language Resources Association, 2022. URL https://aclanthology.org/2022.lrec-1.729.

Hui Wu, Yupeng Gao, Xiaoxiao Guo, Ziad Al-Halah, Steven Rennie, Kristen Grauman, and Rogério Feris. Fashion IQ: A new dataset towards retrieving images by natural language feedback. In *IEEE Conference on Computer Vision and Pattern Recognition, CVPR 2021, virtual, June 19-25, 2021*, pp. 11307–11317. Computer Vision Foundation / IEEE, 2021. doi: 10.1109/CVPR46437.2021.01115. URL https://openaccess.thecvf.com/content/CVPR2021/html/Wu_Fashion_IQ_A_New_Dataset_Towards_Retrieving_Images_by_Natural_CVPR_2021_paper.html.

Jianxiong Xiao, James Hays, Krista A. Ehinger, Aude Oliva, and Antonio Torralba. SUN database: Large-scale scene recognition from abbey to zoo. In *The Twenty-Third IEEE Conference on Computer Vision and Pattern Recognition, CVPR 2010, San Francisco, CA, USA, 13-18 June 2010*, pp. 3485–3492. IEEE Computer Society, 2010. doi: 10.1109/CVPR.2010.5539970. URL https://doi.org/10.1109/CVPR.2010.5539970.

Junbin Xiao, Xindi Shang, Angela Yao, and Tat-Seng Chua. Next-qa: Next phase of question-answering to explaining temporal actions. In *IEEE Conference on Computer Vision and Pattern Recognition, CVPR 2021, virtual, June 19-25, 2021*, pp. 9777–9786. Computer Vision Foundation / IEEE, 2021. doi: 10.1109/CVPR46437.2021.00965. URL https://openaccess.thecvf.com/content/CVPR2021/html/Xiao_NExT-QA_Next_Phase_of_Question-Answering_to_Explaining_Temporal_Actions_CVPR_2021_paper.html.

Jun Xu, Tao Mei, Ting Yao, and Yong Rui. MSR-VTT: A large video description dataset for bridging video and language. In *2016 IEEE Conference on Computer Vision and Pattern Recognition,*

CVPR 2016, Las Vegas, NV, USA, June 27-30, 2016, pp. 5288–5296. IEEE Computer Society, 2016. doi: 10.1109/CVPR.2016.571. URL https://doi.org/10.1109/CVPR.2016.571.

Xiao Xu, Bei Li, Chenfei Wu, Shao-Yen Tseng, Anahita Bhiwandiwalla, Shachar Rosenman, Vasudev Lal, Wanxiang Che, and Nan Duan. Managertower: Aggregating the insights of uni-modal experts for vision-language representation learning. In Anna Rogers, Jordan L. Boyd-Graber, and Naoaki Okazaki (eds.), *Proceedings of the 61st Annual Meeting of the Association for Computational Linguistics (Volume 1: Long Papers), ACL 2023, Toronto, Canada, July 9-14, 2023*, pp. 14507–14525. Association for Computational Linguistics, 2023a. doi: 10.18653/V1/2023.ACL-LONG.811. URL https://doi.org/10.18653/v1/2023.acl-long.811.

Xiao Xu, Chenfei Wu, Shachar Rosenman, Vasudev Lal, Wanxiang Che, and Nan Duan. Bridgetower: Building bridges between encoders in vision-language representation learning. In Brian Williams, Yiling Chen, and Jennifer Neville (eds.), *Thirty-Seventh AAAI Conference on Artificial Intelligence, AAAI 2023, Thirty-Fifth Conference on Innovative Applications of Artificial Intelligence, IAAI 2023, Thirteenth Symposium on Educational Advances in Artificial Intelligence, EAAI 2023, Washington, DC, USA, February 7-14, 2023*, pp. 10637–10647. AAAI Press, 2023b. doi: 10.1609/AAAI.V37I9.26263. URL https://doi.org/10.1609/aaai.v37i9.26263.

Shi Yu, Chaoyue Tang, Bokai Xu, Junbo Cui, Junhao Ran, Yukun Yan, Zhenghao Liu, Shuo Wang, Xu Han, Zhiyuan Liu, and Maosong Sun. Visrag: Vision-based retrieval-augmented generation on multi-modality documents. In *The Thirteenth International Conference on Learning Representations, ICLR 2025, Singapore, April 24-28, 2025*. OpenReview.net, 2025. URL https://openreview.net/forum?id=zG459X3Xge.

Zhou Yu, Dejing Xu, Jun Yu, Ting Yu, Zhou Zhao, Yueting Zhuang, and Dacheng Tao. Activitynet-qa: A dataset for understanding complex web videos via question answering. In *The Thirty-Third AAAI Conference on Artificial Intelligence, AAAI 2019, The Thirty-First Innovative Applications of Artificial Intelligence Conference, IAAI 2019, The Ninth AAAI Symposium on Educational Advances in Artificial Intelligence, EAAI 2019, Honolulu, Hawaii, USA, January 27 - February 1, 2019*, pp. 9127–9134. AAAI Press, 2019. doi: 10.1609/AAAI.V33I01.33019127. URL https://doi.org/10.1609/aaai.v33i01.33019127.

Huaying Yuan, Jian Ni, Yueze Wang, Junjie Zhou, Zhengyang Liang, Zheng Liu, Zhao Cao, Zhicheng Dou, and Ji-Rong Wen. Momentseeker: A comprehensive benchmark and A strong baseline for moment retrieval within long videos. *CoRR*, abs/2502.12558, 2025. doi: 10.48550/ARXIV.2502.12558. URL https://doi.org/10.48550/arXiv.2502.12558.

Biao Zhang and Rico Sennrich. Root mean square layer normalization. In Hanna M. Wallach, Hugo Larochelle, Alina Beygelzimer, Florence d'Alché-Buc, Emily B. Fox, and Roman Garnett (eds.), *Advances in Neural Information Processing Systems 32: Annual Conference on Neural Information Processing Systems 2019, NeurIPS 2019, December 8-14, 2019, Vancouver, BC, Canada*, pp. 12360–12371, 2019. URL https://proceedings.neurips.cc/paper/2019/hash/1e8a19426224ca89e83cef47f1e7f53b-Abstract.html.

Xin Zhang, Yanzhao Zhang, Wen Xie, Mingxin Li, Ziqi Dai, Dingkun Long, Pengjun Xie, Meishan Zhang, Wenjie Li, and Min Zhang. GME: improving universal multimodal retrieval by multimodal llms. *CoRR*, abs/2412.16855, 2024. doi: 10.48550/ARXIV.2412.16855. URL https://doi.org/10.48550/arXiv.2412.16855.

Bolei Zhou, Àgata Lapedriza, Aditya Khosla, Aude Oliva, and Antonio Torralba. Places: A 10 million image database for scene recognition. *IEEE Trans. Pattern Anal. Mach. Intell.*, 40(6):1452–1464, 2018a. doi: 10.1109/TPAMI.2017.2723009. URL https://doi.org/10.1109/TPAMI.2017.2723009.

Luowei Zhou, Nathan Louis, and Jason J. Corso. Weakly-supervised video object grounding from text by loss weighting and object interaction. In *British Machine Vision Conference 2018, BMVC 2018, Newcastle, UK, September 3-6, 2018*, pp. 50. BMVA Press, 2018b. URL http://bmvc2018.org/contents/papers/0070.pdf.

Yuke Zhu, Oliver Groth, Michael S. Bernstein, and Li Fei-Fei. Visual7w: Grounded question answering in images. In *2016 IEEE Conference on Computer Vision and Pattern Recognition, CVPR 2016, Las Vegas, NV, USA, June 27-30, 2016*, pp. 4995–5004. IEEE Computer Society, 2016. doi: 10.1109/CVPR.2016.540. URL https://doi.org/10.1109/CVPR.2016.540.

Tianyu Zong, Bingkang Shi, Hongzhu Yi, and Jungang Xu. TNCSE: tensor norm constraints for unsupervised contrastive learning of sentence embeddings. In Toby Walsh, Julie Shah, and Zico Kolter (eds.), *AAAI-25, Sponsored by the Association for the Advancement of Artificial Intelligence, February 25 - March 4, 2025, Philadelphia, PA, USA*, pp. 26192–26201. AAAI Press, 2025. doi: 10.1609/AAAI.V39I24.34816. URL https://doi.org/10.1609/aaai.v39i24.34816.

A Analysis of Parameters for $\frac{\partial L_{TN}(k,t)}{\partial t}$

The partial derivative of $L_{TN}(k,t)$ with respect to t is given by

$$\frac{\partial L_{TN}(k,t)}{\partial t} = -\frac{k}{1+k} \cdot \frac{1}{\sqrt{1+k^2-2kt}}, \tag{A-1}$$

where the domain is defined as $k \in [0, +\infty)$ and $t \in [-1, 1]$. Observe that for all $k > 0$, the prefactor $-\frac{k}{1+k} < 0$, and at $k = 0$, the derivative vanishes (a trivial case). Thus, the sign of $\frac{\partial L_{TN}(k,t)}{\partial t}$ is entirely governed by the term:

$$h(k,t) = \frac{1}{\sqrt{f(k,t)}}, \quad \text{where} \quad f(k,t) = 1 + k^2 - 2kt. \tag{A-2}$$

Since $h(k,t)$ involves a square root in the denominator, we require $f(k,t) > 0$ for well-definedness. We now analyze where $f(k,t) = 0$ within the domain $k \geq 0,\ t \in [-1, 1]$.

Treat $f(k,t)$ as a quadratic in k with parameter $t \in [-1, 1]$:

$$f(k,t) = k^2 - 2tk + 1.$$

Its discriminant is

$$\Delta = (-2t)^2 - 4 \cdot 1 \cdot 1 = 4(t^2 - 1).$$

We consider the following cases:

- **Case 1:** $\Delta > 0$, i.e., $|t| > 1$. This implies two distinct real roots in k, but such values of t lie outside the domain $[-1, 1]$. Hence, no solutions exist in the feasible region.
- **Case 2:** $\Delta = 0$, i.e., $t = \pm 1$.
  - If $t = 1$, then $f(k, 1) = (k-1)^2$, which vanishes when $k = 1$. Thus, $(k,t) = (1, 1)$ is a zero of $f(k,t)$.
  - If $t = -1$, then $f(k, -1) = (k+1)^2$, which vanishes when $k = -1$. However, since $k \geq 0$, this point lies outside the domain and is discarded.
- **Case 3:** $\Delta < 0$, i.e., $|t| < 1$. Then $f(k,t) > 0$ for all $k \in [0, +\infty)$, meaning no real roots exist and the expression under the square root remains strictly positive.

Therefore, the only point in the domain where $f(k,t) = 0$ is $(k,t) = (1, 1)$. Consequently,

- $f(k,t) > 0$ for all $(k,t) \in [0, +\infty) \times [-1, 1] \setminus \{(1, 1)\}$;
- At $(1, 1)$, $f(k,t) \to 0^+$, causing $\frac{1}{\sqrt{f(k,t)}} \to +\infty$, and thus $\frac{\partial L_{TN}(k,t)}{\partial t} \to -\infty$.

Hence, $\frac{\partial L_{TN}(k,t)}{\partial t}$ has a *single isolated infinite discontinuity* at $(k,t) = (1, 1)$, and is strictly negative everywhere else in the domain:

$$\frac{\partial L_{TN}(k,t)}{\partial t} < 0, \quad \forall (k,t) \in [0, +\infty) \times [-1, 1] \setminus \{(1, 1)\}. \tag{A-3}$$

This implies that, for any fixed $k > 0$ with $k \neq 1$, the function $L_{TN}(k,t)$ is strictly decreasing in t over $[-1, 1)$. Although the derivative is undefined at $(1, 1)$, we verify that $L_{TN}(k,t)$ itself remains continuous at this point (by direct substitution into the original loss function). Therefore, the minimum value of $L_{TN}(k,t)$ with respect to t occurs at the right endpoint $t = 1$, for all $k > 0$.

For all $k > 0$, the function $L_{TN}(k,t)$ attains its global minimum over $t \in [-1, 1]$ at $t = 1$, despite the singularity in the derivative at $(k,t) = (1, 1)$.

The discontinuity in the derivative does not affect the existence or location of the minimum because the function $L_{TN}(k,t)$ is continuous on the closed domain $[0, +\infty) \times [-1, 1]$. The monotonicity holds almost everywhere, and the endpoint $t = 1$ remains the unique minimizer by continuity and boundary analysis.

This result justifies our choice of $t = 1$ as the optimal setting in the training objective, ensuring stability and convergence properties in the optimization landscape.

B Differences Between Reproduced Results of VLM2Vec-V2 for Full Tasks and the Original Paper

We first acknowledge the open-source release of VLM2Vec-V2. In the original VLM2Vec-V2 paper, the authors report an average performance of 65.4 on the Hit@1 metric for the VisDoc task across the full-task training set. However, in our work, we reproduce the results using the same hardware configuration as the original paper and strictly follow its open-source code with default hyperparameters. Our results are only 61.1[6], significantly lower than the original reported value, multiple issues in the official code repository report similar reproduction failures[7][8]. Currently, we and our peers preliminarily speculate that this inconsistency may stem from version differences in the DATASETS package. There may be implicit behavioral changes in data loading, sampling order, or preprocessing workflows across different versions of the datasets package[9], which could affect the stability of model training and evaluation. However, as of the submission of this paper, the official repository for VLM2Vec-V2 still does not explicitly specify the exact versions of its dependencies. To ensure fairness and comparability in experimental evaluation, we still adopt the currently reproducible baseline result as the comparison baseline. Our method achieves superior performance under identical training and evaluation environments, leading to a reasonable inference: compared to the current implementation of VLM2Vec-V2, our approach inherently demonstrates greater effectiveness and robustness. We report the results of the original VLM2Vec-V2 paper and our reproduction in Table B-1 and compare them with our proposed TNCME. We commit to retraining and reevaluating our method in an environment that can reproduce the original results, and to reporting the results in our open-source repository if this reproducibility issue is resolved in the future. We once again sincerely thank the VLM2Vec-V2 team for their valuable contributions to the open-source community.

C Training and Evaluation Datasets

VLM2Vec-V2 constructs a training-evaluation framework for multimodal retrieval tasks called MMEB-V2. The training dataset comprises three categories: image-text, VisDoc-text, and video-text retrieval data. The following table details the sub-datasets and quantities within each dataset category. The MMEB-V2 benchmark test set comprises 81 sub-tasks across three major retrieval task categories, organized under nine meta-tasks. These cover the three primary modalities: images, videos, and visual documents. Completely independent of the training set, this test set measures the model's generalization capabilities. Tables C-1 and C-2 detail the sources and quantities for each task. To uniformly evaluate model performance across multimodal retrieval tasks, we use the average performance across each modality's test set as the evaluation metric.

D Evaluation Metrics

In this section, we summarize the evaluation metrics employed in the task in Table D-1.

[6]The benchmark MMEB-V2, introduced by VLM2Vec-V2, actually encompasses 27 VisDoc tasks. However, VLM2Vec-V2 evaluated only 24 of them, excluding three multilingual tasks. In our evaluation, we have tested all 27 VisDoc tasks.

[7]https://github.com/TIGER-AI-Lab/VLM2Vec/issues/130

[8]https://github.com/TIGER-AI-Lab/VLM2Vec/issues/149

[9]To avoid breaking double-blind protocols, this is the outcome of our discussions conducted through alternative communication channels rather than via issues in the VLM2Vec-V2 official repository.

Table B-1: We report the original results of VLM2Vec-V2 in this table, including several baselines. We also report our reproduced results for VLM2Vec-V2 under identical conditions, along with the results for TNCME. The evaluation metrics are consistent with the VLM2Vec-V2.

Model	Image (Hit@1) 36 Avg.	Video (Hit@1) 18 Avg.	VisDoc (NDCG@5) 24 Avg.	All	Train Sets
ColPali-v1.3	34.9	28.2	71.0	44.5	Not Reported in VLM2Vec-V2
GME-2B	51.9	33.9	72.7	54.1	
GME-7B	56.0	**38.6**	**75.2**	**57.9**	
LamRA-Qwen2-7B	54.1	35.2	23.9	40.4	
LamRA-Qwen2.5-7B	52.4	33.7	50.2	47.4	
VLM2Vec-Qwen2VL-2B	59.7	29.0	41.6	47.0	
VLM2Vec-Qwen2VL-7B	**65.5**	34.0	46.4	52.4	
VLM2Vec-V2-2B Reported 5k steps	**64.9**	**34.9**	**65.4**	**58.1**	All Sets
VLM2Vec-V2-2B Reproduced 5k steps	64.4	33.4	61.1	56.2	
VLM2Vec-V2-2B Reproduced 2k steps	62.4	35.0	57.9	54.7	All Sets
TNCME-2B 2k steps	**62.8**	**35.2**	**58.1**	**55.0**	
VLM2Vec-V2-2B Reproduced 5k steps	63.7	30.0	29.9	45.5	Image-Text Only
TNCME-2B 2k steps	**64.9**	**31.4**	**31.2**	**46.8**	
VLM2Vec-V2-2B Reproduced 5k steps	64.5	32.9	56.8	54.8	Image-Text & VisDoc-Text
TNCME-2B 2k steps	**65.3**	**33.0**	**57.9**	**55.6**	

Table C-1: Sub-datasets for the Image-Text retrieval tasks and VisDoc-Text retrieval tasks in MMEB-V2.

Task Type	Task Name	Reference
Visual Question Answering	OK-VQA	(Marino et al., 2019)
	A-OKVQA	(Schwenk et al., 2022)
	DocVQA	(Mathew et al., 2021)
	InfoVQA	(Mathew et al., 2022)
	ChartQA	(Masry et al., 2022)
	Visual7W	(Zhu et al., 2016)
	ScienceQA	(Lu et al., 2022)
	GQA	(Hudson & Manning, 2019)
	TextVQA	(Singh et al., 2019)
	VizWiz	(Gurari et al., 2018)
Image Classification	Voc2007	(Everingham et al., 2010)
	N24News	(Wang et al., 2022)
	SUN397	(Xiao et al., 2010)
	ObjectNet	(Barbu et al., 2019)
	Country211	(Radford et al., 2021b)
	Place365	(Zhou et al., 2018a)
	ImageNet-1K	(Russakovsky et al., 2015)
	ImageNet-A	(Hendrycks et al., 2019)
	ImageNet-R	(Hendrycks et al., 2021)
	HatefulMemes	(Kiela et al., 2020)
Image-level Retrieval	MSCOCO_I2T	(Lin et al., 2014)
	MSCOCO_T2I	(Lin et al., 2014)
	VisDial	(Das et al., 2017)
	CIRR	(Liu et al., 2021b)
	VisualNews I2T	(Liu et al., 2021a)
	VisualNews T2I	(Liu et al., 2021a)
	NIGHTS	(Diament et al., 2023)
	WebQA	(Chang et al., 2022)
	EDIS	(Liu et al., 2023b)
	OVEN	(Hu et al., 2023)
	WIKI-SS-NQ	(Ma et al., 2024a)
	FashionIQ	(Wu et al., 2021)
Visual Document Retrieval	ViDoRe	(Faysse et al., 2025b)
	ViDoRe-v2	(Macé et al., 2025)
	VisRAG	(Yu et al., 2025)
	ViDoSeek	(Wang et al., 2025a)
	MMLongBench-Doc	(Ma et al., 2024b)
Visual Grounding	MSCOCO	(Lin et al., 2014)
	RefCOCO	(Kazemzadeh et al., 2014)
	RefCOCO-Matching	-
	Visual7W-Pointing	(Zhu et al., 2016)

Table C-2: Sub-datasets for the VisDoc-Text retrieval tasks in MMEB-V2.

Task Type	Task Name	Reference
Video Question Answering	Video-MME	(Fu et al., 2025)
	MVBench	(Li et al., 2024)
	NExT-QA	(Xiao et al., 2021)
	EgoSchema	(Mangalam et al., 2023)
	ActivityNetQA	(Yu et al., 2019)
Video Classification	UCF101	(Soomro et al., 2012)
	HMDB51	(Kuehne et al., 2011)
	Kinetics-700	(Carreira et al., 2019)
	Breakfast	(Kuehne et al., 2014)
	Something-Something V2	(Goyal et al., 2017)
Video-level Retrieval	MSR-VTT	(Xu et al., 2016)
	MSVD	(Chen & Dolan, 2011)
	DiDeMo	(Hendricks et al., 2017)
	VATEX	(Wang et al., 2019)
	YouCook2	(Zhou et al., 2018b)
Moment Retrieval	QVHighlights	(Lei et al., 2021)
	Charades-STA	(Gao et al., 2017)
	MomentSeeker	(Yuan et al., 2025)

Table D-1: Evaluation Metrics and Their Meanings

Metric	Description
Hit@K	Proportion of queries where the correct item is ranked within top-K.
NDCG@K	Normalized ranking quality; supports linear (0/1) or exponential ($2^{\text{rel}} - 1$) relevance gain.
Precision@K	Fraction of retrieved top-K items that are relevant.
Recall@K	Fraction of all relevant items retrieved in top-K.
F1@K	Harmonic mean of Precision@K and Recall@K.
MAP@K	Mean of Average Precision across queries, truncated at rank K.
MRR@K	Mean reciprocal rank of the first relevant item (capped at K).